

University of Groningen

Computing Contour Generators of Evolving Implicit Surfaces

Plantinga, Simon; Vegter, Geert

Published in:
Acm transactions on graphics

IMPORTANT NOTE: You are advised to consult the publisher's version (publisher's PDF) if you wish to cite from it. Please check the document version below.

Document Version
Publisher's PDF, also known as Version of record

Publication date:
2006

[Link to publication in University of Groningen/UMCG research database](#)

Citation for published version (APA):
Plantinga, S., & Vegter, G. (2006). Computing Contour Generators of Evolving Implicit Surfaces. Acm transactions on graphics, 25(4), 1243-1280.

Copyright

Other than for strictly personal use, it is not permitted to download or to forward/distribute the text or part of it without the consent of the author(s) and/or copyright holder(s), unless the work is under an open content license (like Creative Commons).

Take-down policy

If you believe that this document breaches copyright please contact us providing details, and we will remove access to the work immediately and investigate your claim.

Downloaded from the University of Groningen/UMCG research database (Pure): <http://www.rug.nl/research/portal>. For technical reasons the number of authors shown on this cover page is limited to 10 maximum.

Computing Contour Generators of Evolving Implicit Surfaces

SIMON PLANTINGA and GERT VEGTER
University of Groningen

The contour generator is an important visibility feature of a smooth object seen under parallel projection. It is the curve on the surface which separates front-facing from back-facing regions. The apparent contour is the projection of the contour generator onto a plane perpendicular to the view direction. Both curves play an important role in computer graphics.

Our goal is to obtain fast and robust algorithms that compute the contour generator with a guarantee of topological correctness. To this end, we first study the singularities of the contour generator and apparent contour for both generic views and generic time-dependent projections, for example, when the surface is rotated or deformed. The singularities indicate when components of the contour generator merge or split as time evolves.

We present an algorithm to compute an initial contour generator by using a dynamic step size. An interval test guarantees the topological correctness. This initial contour generator can thus be maintained under a time-dependent projection by examining its singularities.

Categories and Subject Descriptors: I.3.3 [**Computer Graphics**]: Picture/Image Generation—*Line and curve generation*; I.3.5 [**Computer Graphics**]: Computational Geometry and Object Modeling—*Geometric algorithms, languages, and systems*; G.1.0 [**Numerical Analysis**]: General—*Interval arithmetic*

General Terms: Algorithms, Theory

Additional Key Words and Phrases: Implicit surfaces, contour generators, silhouette, contour, guaranteed topology, interval arithmetic, singularities, evolving surfaces

1. INTRODUCTION

An important visibility feature of a smooth object seen under parallel projection along a certain direction is its *contour generator*, also known as outline or profile. The contour generator is the curve on the surface that separates front-facing regions from back-facing regions. This curve may have singularities if the direction of projection is nongeneric. The *apparent* contour is the projection of the contour generator onto a plane perpendicular to the view direction. In many cases, drawing just the visible part of the apparent contour gives a good impression of the shape of the object. In this article, we will not distinguish between visible and invisible parts of the contour generator. Stated otherwise, we assume the surface is transparent. Generically, the apparent contour is a smooth curve with some isolated singularities (see Figure 1).

This work is partially supported by the IST Programme of the EU as a Shared-Cost RTD (FET Open) Project under Contract No. IST-2000-26473 (ECG—Effective Computational Geometry for Curves and Surfaces).

Author's addresses: S. Plantinga and G. Vegter, Institute for Mathematics and Computing Science, University of Groningen, Nijenborgh 4, NL-9747 AG Groningen, The Netherlands; email: simon@cs.rug.nl.

Permission to make digital or hard copies of part or all of this work for personal or classroom use is granted without fee provided that copies are not made or distributed for profit or direct commercial advantage and that copies show this notice on the first page or initial screen of a display along with the full citation. Copyrights for components of this work owned by others than ACM must be honored. Abstracting with credit is permitted. To copy otherwise, to republish, to post on servers, to redistribute to lists, or to use any component of this work in other works requires prior specific permission and/or a fee. Permissions may be requested from Publications Dept., ACM, Inc., 2 Penn Plaza, Suite 701, New York, NY 10121-0701 USA, fax +1 (212) 869-0481, or permissions@acm.org.

© 2006 ACM 0730-0301/06/1000-1243 \$5.00

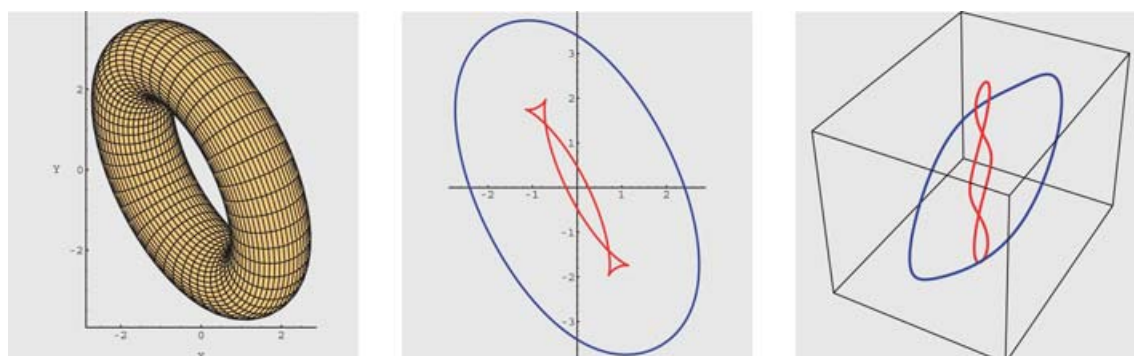


Fig. 1. A smooth surface (left), its apparent contour under parallel projection along the z direction (middle), and its contour generator, seen from a different position (right). For generic surfaces (or generic parallel projections), the contour generator is a smooth, possibly disconnected curve on the surface, whereas the apparent contour may have isolated cusp points.

The contour generator and apparent contour plays important role in computer graphics and computer vision. Rendering a polyhedral model of a smooth surface yields a jaggy outline unless the triangulation of the surface is finer in a neighbourhood of the contour generator. This observation has led to techniques for view-dependent meshing and refinement techniques (see Alliez et al. [2001]).

Also, to render a smooth surface, it is sufficient to render only that part of the surface with front-facing normals, so the contour generator, being the boundary of the potentially visible part, plays a crucial role here. In nonphotorealistic rendering [Markosian et al. 1997], we just visualize the apparent contour, which is perhaps enhanced by strokes indicating the main curvature directions of the surface. This is also the underlying idea in silhouette rendering of implicit surfaces [Bremer and Hughes 1998]. In computer vision, techniques have been developed for the partial reconstruction of a surface from a sequence of apparent contours corresponding to a discrete set of nearby projection directions. We refer to the work of Cipolla and Giblin [2000] for an overview and good introduction to the mathematics underlying this article. Other applications use silhouette interpolation [Gu et al. 1999] from a precomputed set of silhouettes to obtain the silhouette for an arbitrary projection. In computational geometry, rapid silhouette computation of polyhedral models under perspective projection with moving viewpoints has been achieved by applying suitable preprocessing techniques [Barequet et al. 1999].

This article presents a method for the robust computation of contour generators and apparent contours of implicit surfaces. For an introduction to the use of implicit surfaces for smooth deformable object modeling we refer to Opalach and Maddock [1995] and Bloomenthal [1997].

We first consider generic static views, where both the surface and direction of projection are static. Then we pass to time-dependent views, where the direction of projection changes with time. We derive conditions that locate changes in the topology of the contour generator and apparent contour. It turns out that generically, there are three types of events, or *bifurcations*, leading to such a change in topology. These bifurcations have been studied from a much more advanced mathematical point of view, where they are known under the names *lips*, *beak-to-beak*, and *swallowtail* bifurcation (see also Bruce and Giblin [1985]). For a nice nonmathematical description we refer to the beautiful book by Koenderink [1990]. Also, we refer to Arnol'd [1986] and Bruce [1984] for a sketch of some of the mathematical details related to singularity theory. Arnol'd [1976] contains some of the results of the article in a complex analytic setting. Our approach is somewhere in between the level of

Koenderink's book and the sophisticated mathematical approach. We use only elementary tools, like the Inverse and Implicit Function Theorems, and finite order Taylor expansions. These techniques are used to design algorithms in the same way as the Implicit Function Theorem gives rise to Newton's method.

Most curve tracing algorithms step along the curve using a fixed step size (see e.g., Bremer and Hughes [1998] or Hoffman [1989]). For a good approximation, the user has to choose a step size that is "small enough" to follow the details of the curve. Some algorithms predict a dynamic step size based on the local curvature. Both methods cannot guarantee a correct approximation to the curve. Also, these curve tracing algorithms assume there are no singularities. By examining the singularities before tracing the curve, we can avoid them in the tracing process. For certain functions (e.g., algebraic surfaces) the theory on local models, derived in this article, can be used to trace through the singular points. We developed a condition, based on interval analysis, that guarantees topological correctness of the traced curve.

An overview of the theory of singularities of the contour generator appeared in Plantinga and Vegter [2003]. There, we only presented the main results, together with a topologically correct curve tracing algorithm. In this article we present the full derivation of local models in Sections 5 and 6, and extend Section 8 with details for adjusting the contour generators of time-dependent surfaces. We give more results of an implementation for computing static contour generators (also for nonalgebraic surfaces), and timing results for the 4D process to trace evolving surfaces without using algebraic methods. Finally, we included Appendices B and C to summarize the theory required for the derivation of local models.

This article presents the first explicit conditions for an implicit surface to exhibit generic singularities in the contour generator and its associated apparent contour. The main result of this article is a general framework to examine and approximate the contour generators of implicit surfaces. We present a new derivation of the different types of singularities, together with local models. These local models capture the behavior of the surface at singularities of the contour generator in "simple" expressions. For static surfaces, we derive local models for folds and cusps (Propositions 5.1 and 5.2). For evolving surfaces we have lips, beak-to-beak, and swallowtail bifurcations (Propositions 6.1 and 6.3). Using these local models, we give precise conditions to determine the behavior of the contour generator of an implicit surface. For algebraic surfaces, for example, the local models can be used to classify singularities. As a first step to implementation, we present a new curve tracing algorithm. This is the first curve tracing algorithm that guarantees the topological correctness of the piecewise linear approximation. We implemented this algorithm to produce a topologically correct approximation of the contour generator of static implicit surfaces. As a first step towards approximation of contour generators for dynamic surfaces, we explain how "initial" points can be followed in 4D space. We also give timing results for this process. However, current programming libraries are insufficient for an efficient implementation of generic implicit functions. For special classes, such as algebraic surfaces, more efficient solvers are available.

In Section 2 we present the framework, and discuss the criteria for a point on the contour generator and apparent contour to be regular. Section 3 examines singularities under some time-dependent views, for example, when the viewpoint moves or the surface deforms. In Section 4 we explain the transformation to local models. Section 5 shows in detail how to derive local models near fold and cusp points. In Section 6 we examine contours for time-dependent views. For the implementation, interval analysis is used. A brief overview can be found in Section 7. The algorithm for computing the contour generator is explained in Section 8. Finally, the appendices give an overview of the existing theory used in this article.

2. CONTOUR GENERATOR AND APPARENT CONTOUR

2.1 Contour Generators of Implicit Surfaces

To understand the nature of regular and singular points of the contour generator, and their projections on the apparent contour, we assume that S is given as the zero set of a smooth function $F: \mathbb{R}^3 \rightarrow \mathbb{R}$, so $S = F^{-1}(0)$. *Smooth* means that the required derivatives exist; for most of the results, C^3 will be sufficient. In the section on evolving surfaces, sometimes C^5 is required. Furthermore, we assume that 0 is a regular value of F , that is, the gradient ∇F is nonzero at every point of the surface. The gradient vector $\nabla F(p)$ is the normal of the surface at p , that is, it is normal to the tangent plane of S at p . This tangent plane is denoted by $T_p(S)$. If v is the direction of parallel projection, then the contour generator Γ is the set of points at which the normal to S is perpendicular to the direction of projection, that is, $p \in \Gamma$ iff the following conditions hold:

$$\begin{aligned} F(p) &= 0 \\ \langle \nabla F(p), v \rangle &= 0. \end{aligned} \tag{1}$$

For convenience, we assume throughout the article that $v = (0, 0, 1)$. Then the preceding equations reduce to

$$\begin{aligned} F(x, y, z) &= 0 \\ F_z(x, y, z) &= 0. \end{aligned} \tag{2}$$

Here, and in the sequel, we shall occasionally write F_z instead of $\frac{\partial F}{\partial z}(p)$. We also use notation such as F_x and F_{zz} with a similar meaning.

For arbitrary view directions, the formulae become more complicated. It is more convenient to instead rotate the surface by applying a rotation transformation to the implicit function. Also, a linear skewing transformation can be used. For view direction $(\alpha, \beta, 1)$ we consider the function $F(x - \alpha z, y - \beta z, z)$ and use the inverse skewing to move the approximation of the contour generator back to the original surface.

We assume that S is a generic surface, that is, there are no degenerate singular points on its contour generator. Some functions can yield degenerate contour generators. For example, a cylinder has a 2D contour generator for the view direction along its axis. Using a small perturbation, we can remove these degeneracies. In the case of the cylinder, the 2D contour generator collapses to a 1D curve (see, e.g., Stander and Hart [1997]).

We now derive the conditions for contour generator Γ and apparent contour γ to be regular at a given point. Recall that a curve is regular at a certain point if it has a nonzero tangent vector at this point. The next result gives conditions in terms of the function defining the surface.

PROPOSITION 2.1. (1) *A point $p \in \Gamma$ is a regular point of the contour generator if and only if*

$$F_{zz}(p) \neq 0 \text{ or } \Delta(p) \neq 0, \tag{3}$$

where $\Delta(p)$ is a Jacobian determinant defined by

$$\Delta(p) = \frac{\partial(F, F_z)}{\partial(x, y)} \Big|_p = \begin{vmatrix} F_x(p) & F_y(p) \\ F_{xz}(p) & F_{yz}(p) \end{vmatrix}.$$

(2) *A point $p \in \gamma$ is a regular point of the apparent contour if and only if*

$$F_{zz}(p) \neq 0. \tag{4}$$

PROOF. (1) The condition for p to be regular is

$$\nabla F(p) \wedge \nabla F_z(p) \neq 0.$$

Since $F_z(p) = 0$, a straightforward calculation yields

$$\nabla F(p) \wedge \nabla F_z(p) = F_{zz} \cdot (F_y, -F_x, 0) + \frac{\partial(F, F_z)}{\partial(x, y)} \cdot (0, 0, 1). \quad (5)$$

Here, all derivatives are evaluated at p . Since $\nabla F(p) = (F_x(p), F_y(p), 0) \neq 0$, we see that $(F_y, -F_x, 0)$ and $(0, 0, 1)$ are linearly independent vectors. Therefore, the linear combination of these vectors in the righthand-side of Eq. (5) is zero iff the corresponding scalar coefficients are zero. The necessity and sufficiency of condition (3) is a straightforward consequence of this observation.

(2) Since $\nabla F(p) \neq 0 \in \mathbb{R}^3$, and $F_z(p) = 0$, we see that $(F_x(p), F_y(p)) \neq (0, 0)$. Assuming $F_y(p) \neq 0$, we get

$$\frac{\partial(F, F_z)}{\partial(y, z)} \Big|_p = \begin{vmatrix} F_y & F_z \\ F_{yz} & F_{zz} \end{vmatrix} \Big|_p = F_y(p)F_{zz}(p) \neq 0. \quad (6)$$

Let $p = (x_0, y_0, z_0)$. Then, the Implicit Function Theorem yields locally defined functions $\eta, \zeta : \mathbb{R} \rightarrow \mathbb{R}$, with $\eta(x_0) = y_0$ and $\zeta(x_0) = z_0$, such that Eq. (2) holds iff $y = \eta(x)$ and $z = \zeta(x)$. The contour generator is a regular curve parametrized as $x \mapsto (x, \eta(x), \zeta(x))$ locally near p , whereas the apparent contour is a regular curve in the plane parametrized as $x \mapsto (x, \eta(x))$ locally near (x_0, y_0) . \square

2.2 Singular Points of Contour Generators

We apply the preceding result to detect the nondegenerate singularities of contour generators of implicit surfaces. This result will be applied later in this section when we consider the contour generators of time-dependent surfaces.

Again, let the regular surface S be the zero set of a C^3 -function $F : \mathbb{R}^3 \rightarrow \mathbb{R}$, for which 0 is a regular value. We consider the contour generator Γ of S under parallel projection along the vector $v = (0, 0, 1)$. The equations for Γ are

$$F = F_z = 0.$$

We consider the contour generator as the zero set of the function F_z , restricted to S .

COROLLARY 2.2. *Point p is a nondegenerate singular point of Γ iff the following two conditions hold:*

$$F(p) = F_z(p) = F_{zz}(p) = \frac{\partial(F, F_z)}{\partial(x, y)} \Big|_p = 0, \quad (7)$$

and $\Sigma(p) \neq 0$, where for $F_x(p) \neq 0$,

$$\begin{aligned} \Sigma(p) = & -F_x^2 F_{xzz}^2 F_y^2 + 2F_x^3 F_{xzz} F_y F_{yzz} - F_x^4 F_{yzz}^2 \\ & - 2F_x^3 F_{xyz} F_y F_{zzz} + 2F_x^2 F_{xy} F_{xz} F_y F_{zzz} \\ & + F_x^2 F_{xxz} F_y^2 F_{zzz} - F_x F_{xx} F_{xz} F_y^2 F_{zzz} \\ & - F_x^3 F_{xz} F_{yy} F_{zzz} + F_x^4 F_{yyz} F_{zzz}, \end{aligned} \quad (8)$$

whereas for $F_y(p) \neq 0$, we have

$$\begin{aligned} \Sigma(p) = & -F_{xzz}^2 F_y^4 + 2F_x F_{xzz} F_y^3 F_{yzz} - F_x^2 F_y^2 F_{yzz}^2 \\ & - 2F_x F_{xyz} F_y^3 F_{zzz} + F_{xxz} F_y^4 F_{zzz} \\ & + F_x^2 F_y^2 F_{yyz} F_{zzz} + 2F_x F_{xy} F_y^2 F_{yz} F_{zzz} \\ & - F_{xx} F_y^3 F_{yz} F_{zzz} - F_x^2 F_y F_{yy} F_{yz} F_{zzz}. \end{aligned} \quad (9)$$

PROOF. Condition (7) reflects the fact that p is a singular point of $F_z|S$ (see Eq. (3)), whereas Eq. (8) expresses nondegeneracy of this singular point. Condition (8) is obtained by a straightforward expansion¹ of Eq. (46) (see Appendix A) with $G = F_z$ and $V = X$, as in Eq. (47), where $\lambda = \frac{F_{xz}^0}{F_x^0}$, $F_z^0 = F_{zz}^0 = 0$, and $F_{yz}^0 = \frac{F_y^0}{F_x^0} F_{xz}^0$. Condition (9) is derived similarly. \square

2.3 Generic Projections: Fold and Cusp Points

In view of Proposition 2.1, regular points of the apparent contour are projections of points $(x, y, z) \in \mathbb{R}^3$ satisfying

$$F(x, y, z) = F_z(x, y, z) = 0, \quad \text{and} \quad F_{zz}(x, y, z) \neq 0.$$

This being a system of two equations in three unknowns, we expect that the regular points of the apparent contour form a 1D subset of the plane. Furthermore, the singular points of the apparent contour are projections of points satisfying an additional equation, namely, $F_{zz}(x, y, z) = 0$, and are therefore expected to be isolated. This is true for *generic* surfaces. To make this more precise, we consider the set of functions $F : \mathbb{R}^3 \rightarrow \mathbb{R}$ satisfying

$$(F(x, y, z), F_z(x, y, z), F_{zz}(x, y, z), \Delta(x, y, z)) \neq (0, 0, 0, 0), \quad (10)$$

and

$$(F(x, y, z), F_z(x, y, z), F_{zz}(x, y, z), F_{zzz}(x, y, z)) \neq (0, 0, 0, 0). \quad (11)$$

If F satisfies Eq. (10), then Proposition 2.1 tells us that the contour generator Γ of $S = F^{-1}(0)$ under parallel projection along v is a regular curve. Moreover, for a point $(x, y, z) \in \Gamma$ there are two cases:

- (1) $F_{zz}(x, y, z) \neq 0$; in this case, the point projects to a regular point (x, y) of the apparent contour γ . Such a point is called a *fold* point of the contour generator. This terminology is justified by the *local model* of the surface near a fold point, namely,

$$x + z^2 = 0. \quad (12)$$

(see also Figure 2(a)). Here the contour generator is the y -axis in three space, so the apparent contour is the y -axis in the image plane.

- (2) $F_{zz}(x, y, z) = 0$; in this case, the point projects to a singular point (x, y) of γ . Such a point is called a *cusp point* of the contour generator if, in addition to (10), condition (11) is satisfied, that is, if both $\Delta(x, y, z) \neq 0$ and $F_{zzz}(x, y, z) \neq 0$. In this case, the surface has the following local model near the cusp point:

$$G(x, y, z) = x + yz + z^3 = 0. \quad (13)$$

¹Using a computer algebra system.

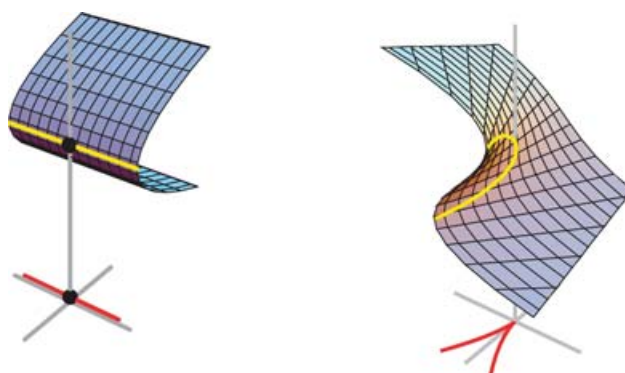


Fig. 2. (a) A local model of the surface at a fold point is $x + z^2 = 0$. Both the contour generator Γ and the visible contour γ are regular at the fold point and its projection onto the image plane, respectively. (b) A local model at a cusp point is $x + yz + z^3 = 0$. Here the contour generator is regular, but the apparent contour has a regular cusp.

(see also Figure 2(b)). The local model G is sufficiently simple to allow for an explicit computation of its contour generator and apparent contour: The former is parametrized by $z \mapsto (2z^3, -3z^2, z)$, while the latter is a *regular cusp* parametrized by $z \mapsto (2z^3, -3z^2)$.

Intuitively speaking, a local model of the surface near a point is a “simple” expression of the defining equation in suitably chosen local coordinates. Usually, as in the cases of fold and cusp points, a local model is a low-degree polynomial, which can be easily analyzed in the sense that the contour generator and apparent contour are easily determined.

Thus, we have only considered parallel projection. The standard perspective transformation Hearn and Baker [1994], which moves the viewpoint to ∞ , reduces perspective projections to parallel projections. By deforming the surface using this transformation, the perspective projections can be computed by using parallel projection on the transformed implicit function. Note that this perspective transform does not influence the smoothness of the implicit surface function.

3. EVOLVING CONTOURS

As we have seen, generic surfaces satisfy conditions (10) and (11), since a violation of one of these conditions would correspond to the existence of a solution of four equations in three unknowns. However, *evolving surfaces* depend on an additional variable, say t . Evolving surfaces occur, for example, when the viewpoint moves along a predetermined path, but also under deformation (or morphing) of the surface. Time dependency is expressed by considering implicitly defined surfaces

$$S_t = \{(x, y, z) \in \mathbb{R}^3 \mid F(x, y, z, t) = 0\},$$

where $F : \mathbb{R}^3 \times \mathbb{R} \rightarrow \mathbb{R}$ is a smooth function of the space variables (x, y, z) and time t . Generically, we expect that exactly one of the conditions (10) and (11) will be violated at isolated values of (x, y, z, t) . For clarity, we assume $(0, 0, 0, 0)$ is such a value.

Violation of Eq. (10) corresponds to a singularity of the contour generator. In this case the implicit surfaces, defined by $F(x, y, z, 0) = 0$ and $F_z(x, y, z, 0) = 0$, are tangent at $(x, y, z) = (0, 0, 0)$, but the tangency is nondegenerate. Stated otherwise, the function $G : \mathbb{R}^3 \rightarrow \mathbb{R}$, defined by $G(x, y, z) = F_z(x, y, z)$, *restricted* to the surface S_0 , has a nondegenerate singularity at $(0, 0, 0)$.

Generically, there are two types of bifurcations corresponding to different scenarios for changes in topology of the contour generator. The beak-to-beak bifurcation corresponds to the *merging* or *splitting* of

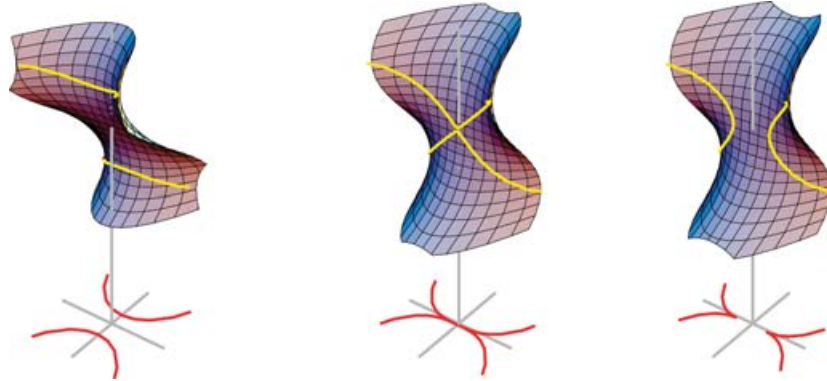


Fig. 3. The beak-to-beak bifurcation. With respect to the local model of Eq. (14) the bifurcation corresponds to $t < 0$ (left), $t = 0$ (middle), and $t > 0$ (right).

connected components of the contour generator. Under some additional generic conditions (inequalities), a local model for this phenomenon is the surface, defined by

$$G(x, y, z, t) = x + (-y^2 + t)z + z^3. \quad (14)$$

Here, the contour generator is defined by $x = 2z^3$, $-y^2 + 3z^2 = -t$, (see also Figure 3).

Having $G^t(x, y, z) = G(x, y, z, t)$, we check that G^0 satisfies Eq. (7) at $p = (0, 0, 0)$, and that $|\Sigma(p)| = -4$ (in fact, $G_x^0 = 1$, so all higher-order derivatives of G_x^0 vanish identically, thus only the last term in the righthand-side of Eq. (8) is not identically equal to zero). Therefore, $G_z^0|S$ has a nondegenerate singular point of saddle type at p . According to the Morse Lemma (see Fomenko and Kunii [1997] or Milnor [1963]), the level set of $G_z^0|S$ through p consists of two regular curves, intersecting transversally at p , which concurs with Figure 3 (middle).

A second scenario due to the violation of Eq. (11) is the lips bifurcation, corresponding to the *birth* or *death* of connected components of the contour generator. Again, under some additional generic conditions, a local model for this phenomenon is the surface, defined by

$$G(x, y, z, t) = x + (y^2 + t)z + z^3. \quad (15)$$

Here, the contour generator is defined by $x = 2z^3$, $y^2 + 3z^2 = -t$. In particular for $t > 0$ the surface S_t has no connected component of the contour generator near $(0, 0, 0)$ and for $t = 0$, the point $(0, 0, 0)$ is isolated on the contour generator. For $t < 0$, there is a small connected component growing out of this isolated point as t decreases beyond 0 (see also Figure 4).

As for the beak-to-beak bifurcation, we show that $G^0|S$ has a nondegenerate singular point at $(0, 0, 0)$, which in this case is an extremum.

Violation of Eq. (11) involves the occurrence of a higher-order singularity of the apparent contour. Note, however, that in this situation the contour generator is still regular at the point (x, y, z) (see Proposition 2.1). Imposing some additional generic conditions a local model for this type of bifurcation is

$$G(x, y, z, t) = x + yz + tz^2 + z^4 = 0. \quad (16)$$

Here, the apparent contour is parametrized as $z \mapsto (tz^2 + z^4, -2tz - 4z^3)$ (see also Figure 5).

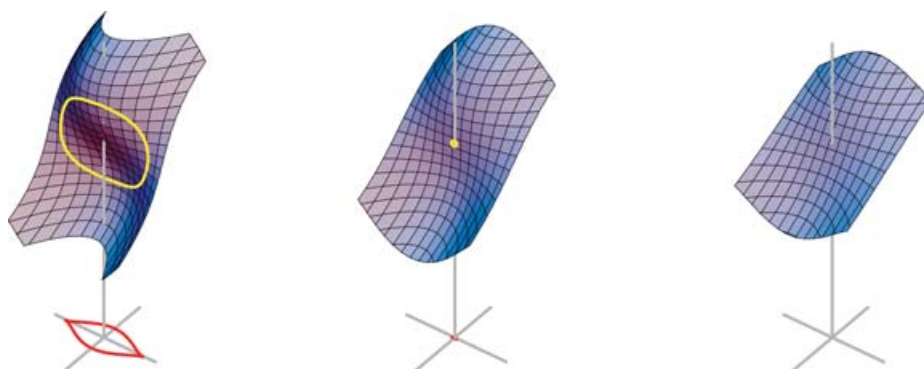


Fig. 4. The lips bifurcation (left: $t < 0$; middle: $t = 0$ right: $t > 0$).

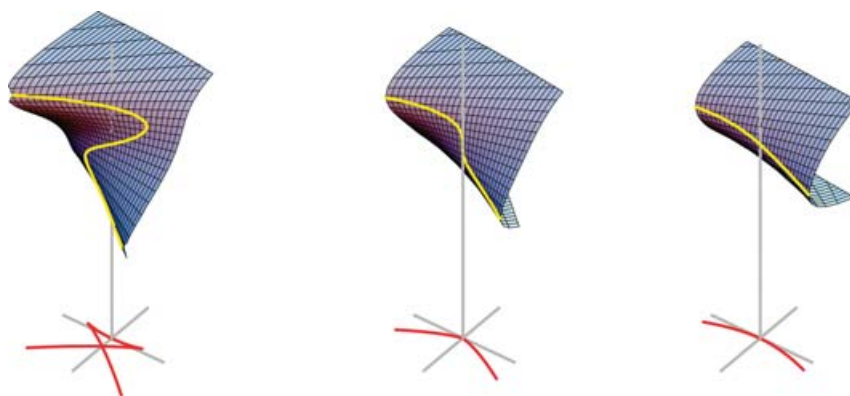


Fig. 5. The swallowtail bifurcation (left: $t < 0$; middle: $t = 0$; right: $t > 0$).

4. TRANSFORMATIONS AND NORMAL FORMS

In Section 2 we presented local models of various types of regular and singular points on contour generators and apparent contours, both for generic static surfaces, and for surfaces evolving generically in time. These local models are low-degree polynomials which are easy to analyze, and yet which capture the *qualitative behavior* of the contour generator and apparent contour in a neighborhood of the point of interest. In this section we explain more precisely what we mean by capturing local behavior.

Consider two regular implicit surfaces $S = F^{-1}(0)$ and $T = G^{-1}(0)$. An invertible smooth map $\Phi: \mathbb{R}^3 \rightarrow \mathbb{R}^3$, for which

$$F \circ \Phi = G \quad (17)$$

maps T to S . In fact, we consider Φ to be defined only locally near some point of T , but we will not express this in our notation. The map Φ need not map the contour generator of T onto that of S , however. To enforce this, we require that Φ maps vertical lines onto vertical lines, that is, Φ should be of the form

$$\Phi(x, y, z) = (h(x, y), H(x, y, z)), \quad (18)$$

where $h: \mathbb{R}^2 \rightarrow \mathbb{R}^2$ and $H: \mathbb{R}^3 \rightarrow \mathbb{R}$ are smooth maps. The map h is even invertible, since Φ is invertible. To allow ourselves even more flexibility in the derivation of local models, we relax condition (17) by

requiring the existence of a nonzero function $\varphi: \mathbb{R}^3 \rightarrow \mathbb{R}$ such that

$$F(\Phi(x, y, z)) = \varphi(x, y, z)G(x, y, z). \quad (19)$$

Definition 4.1. Let $S = F^{-1}(0)$ and $T = G^{-1}(0)$ be regular surfaces near $p = (0, 0, 0) \in \mathbb{R}^3$. An *admissible local transformation* from T to S , locally near p , is a pair (Φ, φ) where $\varphi: \mathbb{R}^3 \rightarrow \mathbb{R}$ is nonzero at p , and $\Phi: \mathbb{R}^2 \times \mathbb{R} \rightarrow \mathbb{R}^3$ is locally invertible near p , and of the form of Eq. (18) such that (19) holds. We also say that Φ brings F in the normal form G .

If the surfaces S and T depend smoothly on k parameters, that is, they are defined by functions $F: \mathbb{R}^3 \times \mathbb{R}^k \rightarrow \mathbb{R}$ and $G: \mathbb{R}^3 \times \mathbb{R}^k \rightarrow \mathbb{R}$, respectively, then we require that the parameters are not mixed with the (x, y, z) -coordinates, that is, we require that Eq. (19) is replaced with

$$F(\Phi(x, y, z, \mu)) = \varphi(x, y, z, \mu)G(x, y, z, \mu),$$

where $\Phi: \mathbb{R}^3 \times \mathbb{R}^k \rightarrow \mathbb{R}^3 \times \mathbb{R}^k$ is of the form

$$\Phi(x, y, z, \mu) = (h(x, y, \mu), H(x, y, z, \mu), \psi(\mu)).$$

Then Φ^μ , defined by $\Phi^\mu(x, y, z) = \Phi(x, y, z, \mu)$, maps T^μ to $S^{\psi(\mu)}$ and preserves contour generators. Furthermore, the map $h^\mu: \mathbb{R}^2 \rightarrow \mathbb{R}^2$, defined by $h^\mu(x, y) = h(x, y, \mu)$, maps the apparent contour of T^μ onto that of $S^{\psi(\mu)}$.

PROPOSITION 4.2. *If Φ is an admissible local transformation from T to S , locally near a point p on the contour generator of T , where Φ is of the form of Eq. (18), then*

- (1) Φ maps T to S , locally near $p \in S$;
- (2) Φ maps the contour generator of T to the contour generator of S , locally near p ;
- (3) h maps the apparent contour of T to the apparent contour of S , locally near the projection $\pi(p) \in \mathbb{R}^2$.

PROOF. From Eqs. (18) and (19) it is easy to derive

$$\begin{aligned} F(\Phi(p)) &= \psi(p)G(p), \\ F_z(\Phi(p))H_z(p) &= \psi_z(p)G(p) + \psi(p)G_z(p). \end{aligned}$$

Since $\psi(p) \neq 0$ and $H_z(p) \neq 0$, we conclude that $G(p) = G_z(p) = 0$ iff $F(\Phi(p)) = F_z(\Phi(p)) = 0$. \square

4.1 Example: Local Model at a Truncated Cusp Point

We now illustrate the use of admissible transformations by deriving a local model for the class of implicit surfaces. These are defined as the zero set of a function of the form:

$$F(x, y, z) = a(x, y) + b(x, y)z + c(x, y)z^2 + z^3, \quad (20)$$

with $a(0, 0) = b(0, 0) = c(0, 0) = 0$, and

$$\left. \frac{\partial(a, b)}{\partial(x, y)} \right|_0 \neq 0. \quad (21)$$

Note that the local model $x + yz + z^3 = 0$, derived in Section 2 for a cusp point, belongs to this class. Our goal is to show that the latter is indeed a local model for all surfaces of the type in Eq.(20). Since $F(0) = F_z(0) = F_{zz}(0) = 0$, and

$$\left. \frac{\partial(F, F_z)}{\partial(x, y)} \right|_0 = \left. \frac{\partial(a, b)}{\partial(x, y)} \right|_0 \neq 0,$$

we see that $0 \in \mathbb{R}^3$ is a regular point of the contour generator of S , whereas $(0, 0)$ is a singular point of the apparent contour (see Proposition 2.1).

As a first step towards a normal form of the implicit surface, we apply the Tschirnhausen transformation $z \mapsto z - \frac{1}{3}c(x, y)$ to transform the quadratic term (in z) in F away. More precisely,

$$\begin{aligned} F(x, y, z - \frac{1}{3}c(x, y)) &= a(x, y) - \frac{1}{3}b(x, y)c(x, y) + \frac{2}{27}c(x, y)^3 + (b(x, y) - \frac{1}{3}c^2(x, y))z + z^3 \\ &= G(\bar{\varphi}(x, y), z), \end{aligned}$$

where $G(x, y, z) = x + yz + z^3$, and

$$\bar{\varphi}(x, y) = (a(x, y) - \frac{1}{3}b(x, y)c(x, y) + \frac{2}{27}c(x, y)^3, b(x, y) - \frac{1}{3}c(x, y)^2).$$

It is not hard to check that the Jacobian determinant of $\bar{\varphi}$ at $0 \in \mathbb{R}^2$ is equal to

$$\left. \frac{\partial(a, b)}{\partial(x, y)} \right|_0,$$

so $\bar{\varphi}$ is a local diffeomorphism near $0 \in \mathbb{R}^2$. Let φ be its inverse. Then, putting

$$\Phi(x, y, z) = (\varphi(x, y), z - \frac{1}{3}c(\varphi(x, y))),$$

we get

$$F \circ \Phi(x, y, z) = G(x, y, z).$$

In other words, the *admissible* transformation Φ brings F into the normal form G . In particular, it maps the surface $T = G^{-1}(0)$ and its contour generator onto $S = F^{-1}(0)$, and φ maps the apparent contour of T onto the apparent contour of S .

5. DERIVING LOCAL MODELS

In this section, we derive local models of an implicit surface near the fold and cusp points of contour generators. The local model for the fold point is as stated in Section 2, while that of the cusp point is slightly weaker in the sense that it includes terms of higher order. To derive these models, we use only elementary means, such as the Implicit Function Theorem and Taylor expansion up to finite order. Although these tools are strong enough to derive the essential qualitative features of the contour generator and apparent contour at a fold or cusp point, they are not strong enough to obtain the simple polynomial form for the cusp, as stated earlier. Although the cubic model for the cusp (see Figure 2b) can be obtained by elementary means, the derivation is quite involved, (see Whitney [1955]). Even worse, the polynomial models of the contour generator of evolving surfaces (see Figures 3, 4, and 5) can only be obtained using sophisticated methods from singularity theory. Therefore, our more modest goal will be to obtain a local model only for the *lower order* part of the implicit function, which is sufficient for our purposes. See Proposition 5.2 for a more precise statement.

5.1 Local Model at a Fold Point

PROPOSITION 5.1. *Let $p \in S$ be a regular point of the contour generator of S , and let its image under parallel projection along v be a regular point of the apparent contour of S . Then there is an admissible transformation, bringing S into the normal form $x \pm z^2 = 0$ (see also Figure 2(a)).*

PROOF. Let $p = 0 \in \mathbb{R}^3$ be a regular point of the contour generator of $S = F^{-1}(0)$, and let its projection $(0, 0)$ be a regular point of the apparent contour. Then, $F(0) = F_z(0) = 0$, and $F_{zz}(0) \neq 0$. Consider F

as a two-parameter family of real-valued univariate functions that depends on the parameters (x, y) , that is,

$$F_{(x,y)}(z) = F(x, y, z).$$

Then, $F_{(0,0)}$ has a nondegenerate singularity at $0 \in \mathbb{R}$, and hence the function $F_{(x,y)}$ has a nondegenerate singularity $z = \zeta(x, y)$, depending smoothly on the parameters (x, y) such that $\zeta(0, 0) = 0$. According to the Morse Lemma with parameters (see Appendix B) there is a local diffeomorphism $(x, y, z) \mapsto (x, y, Z(x, y, z))$ on a neighborhood of $0 \in \mathbb{R}^3$ such that

$$F(x, y, Z(x, y, z)) = \alpha(x, y) \pm z^2,$$

where $\alpha(x, y) = F(x, y, \zeta(x, y))$. Since $(\alpha_x^0, \alpha_y^0) = (F_x^0, F_y^0) \neq (0, 0)$, let us assume that $\alpha_x^0 \neq 0$. Then there is a local diffeomorphism $\varphi : \mathbb{R}^2 \rightarrow \mathbb{R}^2$ of the form $\varphi(x, y) = (\xi(x, y), y)$ such that

$$\alpha(\varphi(x, y)) = x.$$

In fact, $\xi(x, y)$ is the solution of the equation $\alpha(\xi, y) - x = 0$, with $\xi(0, 0) = 0$. The existence and local uniqueness follows from the Implicit Function Theorem. Furthermore, $\xi_x^0 \alpha_x^0 = 1$, which proves that φ is a local diffeomorphism. Therefore,

$$F \circ \Phi(x, y, z) = x \pm z^2,$$

where the local diffeomorphism $\Phi : \mathbb{R}^3 \rightarrow \mathbb{R}^3$ is defined by

$$\Phi(x, y, z) = (\xi(x, y), y, Z(\xi(x, y), y, z)).$$

Now, Φ is an admissible transformation, so it maps the surface T , defined by $x \pm z^2 = 0$, and its contour generator, namely, the line $x = z = 0$, onto S and its contour generator. Furthermore, the diffeomorphism $\varphi : \mathbb{R}^2 \rightarrow \mathbb{R}^2$ maps the apparent contour $x = 0$ of T onto the apparent contour of S . \square

5.2 Local Model at a Cusp Point

PROPOSITION 5.2. *Let $p \in S$ be a point of the contour generator of S , satisfying conditions (10) and (11). Then, p projects onto a cusp point of the apparent contour of S under parallel projection along v . More precisely, there is an admissible transformation, defined on a neighborhood of p , transforming S into a local model of the form*

$$G(x, y, z) = x + yz + z^3 + z^4 R(x, y, z) = 0,$$

where R is a smooth function (see also Figure 2(b)).

Before giving the proof, we observe that this result involves the existence of a map $h : \mathbb{R}^2 \rightarrow \mathbb{R}^2$, that maps the apparent contour of $T = G^{-1}(0)$ onto the apparent contour of $S = F^{-1}(0)$. The apparent contour of T is easily determined by solving x and y from the following system of equations:

$$\begin{aligned} G(x, y, z) &= x + yz + z^3 + z^4 R(x, y, z), \\ G_z(x, y, z) &= y + 3z^2 + z^3(4R(x, y, z) + zR_z(x, y, z)). \end{aligned} \tag{22}$$

Using the Implicit Function Theorem, it is easy to see that we can solve x and y from Eq. (22), yielding

$$\begin{aligned} x(z) &= 2z^3 + O(z^4) \\ y(z) &= -3z^2 + O(z^3). \end{aligned} \tag{23}$$

Therefore, the apparent contour of S has a cusp at $(0, 0)$.

PROOF. We follow the same strategy as in the example of the truncated cusp in Section 4 by transforming the quadratic term of F in z away. For general (not necessarily polynomial) functions F , the Tschirnhausen transformation is obtained as follows. Since $F_{zzz}(p) \neq 0$, the Implicit Function Theorem guarantees that

$$F_{zz}(x, y, z) = 0 \quad (24)$$

has a solution $z = z(x, y)$, locally near $(0, 0)$ with $z(0, 0) = 0$. In this situation, Taylor expansion yields

$$F(x, y, z + z(x, y)) = C(x, y)(U(x, y) + V(x, y)z + z^3 + z^4 R_4(x, y, z)), \quad (25)$$

where R_4 is a smooth function, and

$$\begin{aligned} C(x, y) &= \frac{1}{6} F_{zzz}(x, y, z(x, y)). \\ U(x, y) &= F(x, y, z(x, y))/C(x, y) \\ V(x, y) &= F_z(x, y, z(x, y))/C(x, y). \end{aligned} \quad (26)$$

Note that $C(0, 0) \neq 0$. Furthermore, $U(0, 0) = V(0, 0) = 0$. Note that there is no quadratic term in Eq. (25) because $F_{zz}(x, y, z(x, y)) = 0$.

The righthand-side of Eq. (25) is in fact the form of F after the parameter-dependent change of coordinates $(x, y, z) \mapsto (x, y, z + z(x, y))$. We try to polish (25) further by applying additional admissible transformations of the parameters (x, y) and variable z . To this end, observe that

$$\left. \frac{\partial(U, V)}{\partial(x, y)} \right|_{(0,0)} = \frac{6}{F_{zzz}^0} \left. \frac{\partial(F, F_z)}{\partial(x, y)} \right|_{(0,0)} \neq 0.$$

Therefore, there is an invertible smooth local change of x, y -coordinates $\varphi : \mathbb{R}^2 \rightarrow \mathbb{R}^2$ such that

$$U \circ \varphi(x, y) = x, \quad \text{and} \quad V \circ \varphi(x, y) = y. \quad (27)$$

Therefore

$$F(\varphi(x, y), z + z(\varphi(x, y))) = C(x, y)G(x, y, z),$$

where

$$G(x, y, z) = x + yz + z^3 + z^4 R(x, y, z),$$

with $R(x, y, z) = R_4(\varphi(x, y), z)$. In other words: G is a local model of F . \square

6. TIME-DEPENDENT CONTOURS

If we allow the direction of projection to change over time or equivalently, if we fix the direction of projection and allow the surface to depend on time, the implicit function that defines the surface depends on the four variables (x, y, z, t) , where t corresponds to time. In this situation, we expect one of the conditions (10) and (11) to be violated at isolated values of (x, y, z, t) (see also the description of evolving contours in Section 2). In this section, we derive approximate local models for these degenerate situations (see Figures 3, 4, and 5).

As stated earlier, we consider a smooth function $F : \mathbb{R}^3 \times \mathbb{R} \rightarrow \mathbb{R}$, that defines a time-dependent surface $S_t = (F^t)^{-1}(0)$, where $F^t : \mathbb{R}^3 \rightarrow \mathbb{R}$ is defined by $F^t(x, y, z) = F(x, y, z, t)$.

6.1 Lips and Beak-to-Beak Bifurcations

The occurrence of lips and beak-to-beak bifurcations are associated with a violation of condition (10).

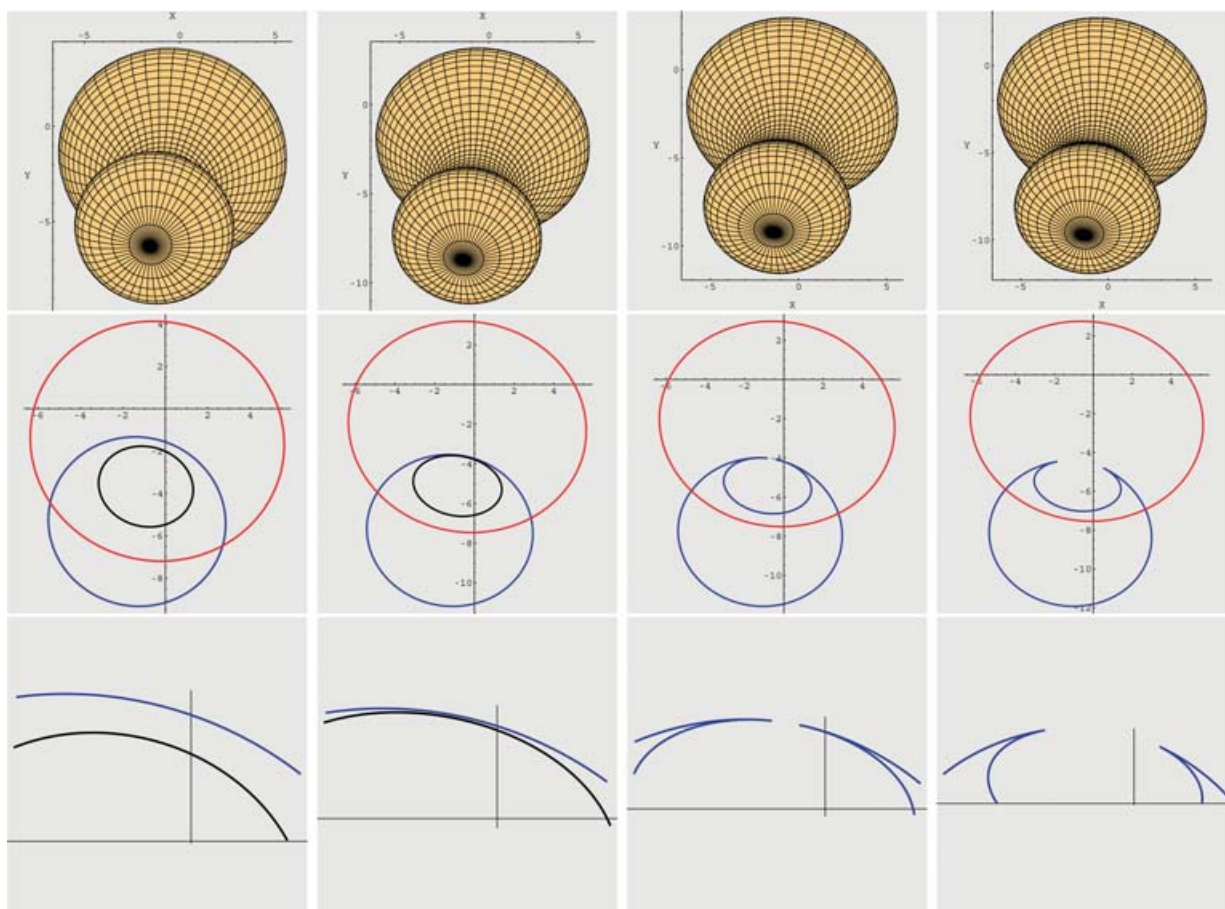


Fig. 6. A beak-to-beak bifurcation. Top row: a sequence of views of a smooth surface. Middle row: the corresponding apparent contours. Bottom row: blow up of the apparent contour near the bifurcation event.

PROPOSITION 6.1. *Let p be a nondegenerate singular point of the contour generator for $t = t_0$, that is,*

$$F(p, t_0) = F_z(p, t_0) = F_{zz}(p, t_0) = \frac{\partial(F, F_z)}{\partial(x, y)} \Big|_{(p, t_0)} = 0, \text{ and } F_{zzz}(p, t_0) \neq 0, \quad (28)$$

and

$$\Sigma(p) \neq 0,$$

where $\Sigma(p)$ is as in Eqs. (8) or (9). Moreover, assume that the matrix

$$\begin{pmatrix} F_x^0 & F_y^0 & F_t^0 \\ F_{xz}^0 & F_{yz}^0 & F_{tz}^0 \end{pmatrix} \text{ has rank two.} \quad (29)$$

Then the surface has a local model at (p, t_0) of the form

$$G(x, y, z, t) = x + (\sigma y^2 + \alpha(x, t))z + z^3 + z^4 R(x, y, z, t),$$

where $\sigma = \text{sign}(\Sigma(p))$ with $\Sigma(p)$ defined by Eqs. (8) or (9), R is a smooth function for (x, y, z, t) near $(0, 0, 0, 0)$, and $\frac{\partial \alpha}{\partial t}(0, 0) \neq 0$.

Remark 6.2. Before giving the proof, we observe that the contour generator is determined by the equations $G = G_z = 0$, that is,

$$\begin{aligned} x + (\sigma y^2 + \alpha(x, y))z + z^3 &= O(z^4), \\ (\sigma y^2 + \alpha(x, y))z + 3z^2 &= O(z^3). \end{aligned}$$

Solving this system for x and y yields

$$\begin{aligned} x &= 2z^3 + O(z^4) \\ \sigma y^2 + 3z^2 &= -\alpha(x, t) + O(z^3). \end{aligned}$$

Since $\alpha(0, 0) = 0$, it is easy to see that the singularity of the contour generator for $t = 0$ is of saddle type if $\sigma = -1$, and corresponds to an extremum if $\sigma = +1$. The former case corresponds to a beak-to-beak bifurcation, the latter to a lips bifurcation. We have a scenario like those depicted in Figures 3 and 4, respectively, where it depends on the sign of $\frac{\partial \alpha}{\partial t}(0, 0)$ whether we have to read the figure from left-to-right or from right-to-left as t passes zero from negative to positive values.

PROOF. For ease of notation we assume that $p = (0, 0, 0)$ and $t_0 = 0$. Our approach is as in the derivation of the local normal form near a cusp point, that is, we again consider the equation

$$F_{zz}(x, y, z, t) = 0 \quad (30)$$

(see Eq. (24)). Since $F_{zzz}(0, 0, 0, 0) \neq 0$, there is a locally unique solution $z = \zeta(x, y, t)$ of Eq. (30), with $\zeta(0, 0, 0) = 0$. Also in this situation, Taylor expansion yields:

$$F(x, y, z + z(x, y), t) = C(x, y, t)U(x, y, t) + V(x, y, t)z + z^3 + z^4 R_4(x, y, z, t),$$

where R_4 is a smooth function, and

$$\begin{aligned} C(x, y, t) &= \frac{1}{6} F_{zzz}(x, y, z(x, y, t)), \\ U(x, y, t) &= F(x, y, z(x, y, t), t) / C(x, y, t) \\ V(x, y, t) &= F_z(x, y, z(x, y, t), t) / C(x, y, t). \end{aligned}$$

Also in this case, $C(0, 0, 0) \neq 0$ and $U(0, 0, 0) = V(0, 0, 0) = 0$. To avoid superscripts, we introduce the functions $u, v : \mathbb{R}^2 \rightarrow \mathbb{R}$, defined by $u(x, y) = U(x, y, 0)$ and $v(x, y) = V(x, y, 0)$. In this case we have

$$\frac{\partial(U, V)}{\partial(x, y)} \Big|_{(0,0)} = \frac{6}{F_{zzz}^0} \frac{\partial(F, F_z)}{\partial(x, y)} \Big|_{(0,0)} = 0, \quad (31)$$

so, unlike the situation at a cusp point, we don't have the normal form (x, y) for the pair (u, v) . Yet, we can obtain a normal form as stated in the proposition. To this end, we introduce the map $\Psi : \mathbb{R}^2 \times \mathbb{R} \rightarrow \mathbb{R}^2$, defined by

$$\Psi(x, y, t) = (U(x, y, t), V(x, y, t)). \quad (32)$$

It follows from Eq. (32) that the Jacobian determinant $J = U_x V_y - U_y V_x$ of Ψ satisfies

$$J(0, 0, 0) = 0. \quad (33)$$

Since, moreover,

$$(u_x^0, u_y^0) = \frac{6}{F_{zzz}^0} (F_x^0, F_y^0) \neq (0, 0), \quad (34)$$

the derivative of the map $\psi : \mathbb{R}^2 \rightarrow \mathbb{R}^2$, defined by $\psi(x, y) = (u(x, y), v(x, y))$ at $(0, 0) \in \mathbb{R}^2$ has rank one.

This observation brings us to the context of singularity theory, in particular, the theory of normal forms of generic maps from plane to plane. Whitney [1955] presents a local normal form for the two types of generic singularities of this type of map namely, the fold and cusp. As said before, although (or perhaps, because) our article uses elementary tools, the technical details are quite involved. We refer the reader to Appendix C for a rather self-contained derivation of the Whitney fold, fine-tuned to our current context.

To make the link with Whitney's result more precise, observe that the Jacobian determinant j of ψ satisfies the identity $j(x, y) = J(x, y, 0)$. Since $\nabla u(0, 0) \neq (0, 0)$ (see Eq. (34)), Proposition C.3, or rather, its parametrized version presented in Section C.3, guarantees the existence of a change of parameters $\varphi(x, y, t)$ of the form $\varphi(x, y, t) = (\cdot, \cdot, t)$ such that

$$U \circ \varphi(x, y, t) = x, \quad \text{and} \quad V \circ \varphi(x, y, t) = \sigma y^2 + \alpha(x, t).$$

Here, α is a smooth function with $\alpha(0, 0) = 0$, and

$$\sigma = \text{sign}(\langle \nabla u(0, 0), \nabla j(0, 0)^\perp \rangle) = \text{sign}(-u_x^0 j_y^0 + u_y^0 j_x^0).$$

A straightforward, but tedious—hence preferably automated—computation shows that

$$-u_x^0 j_y^0 + u_y^0 j_x^0 = \Sigma(p),$$

where $\Sigma(p)$ is defined by Eqs. (8) or (9). Therefore,

$$F(\varphi(x, y, t), z + z(\varphi(x, y, t))) = C(x, y, t)G(x, y, z, t),$$

where

$$G(x, y, z) = x + (\sigma y^2 + \alpha(x, t))z + z^3 + z^4 R(x, y, z)$$

with $R(x, y, z) = R_4(\varphi(x, y, t), z)$. In other words: G is a local model of F . \square

6.2 The Swallowtail Bifurcation

In this section we study the discontinuous change of the apparent contour associated with a violation of Eq. (11), whereas (10) still holds. In this case the contour generator is regular.

PROPOSITION 6.3. *Let $F : \mathbb{R}^3 \times \mathbb{R} \rightarrow \mathbb{R}$ be such that at $(p, t_0) \in \mathbb{R}^3 \times \mathbb{R}$ the following conditions are satisfied:*

$$F(p, t_0) = F_z(p, t_0) = F_{zz}(p, t_0) = F_{zzz}(p, t_0) = 0. \quad (35)$$

If at (p, t_0) the generic conditions

$$F_{zzzz}(p, t_0) \neq 0, \quad \left. \frac{\partial(F, F_z)}{\partial(x, y)} \right|_{(p, t_0)} \neq 0, \quad \text{and} \quad \left. \frac{\partial(F, F_z, F_{zz})}{\partial(x, y, t)} \right|_{(p, t_0)} \neq 0 \quad (36)$$

are satisfied, then F has a local model at (p, t_0) of the form

$$G(x, y, z, t) = x + yz + w(x, y, t)z^2 + z^4 + z^5 R(x, y, z, t) \quad (37)$$

with $w(0, 0, t) = \alpha t + O(t^2)$, where

$$\alpha = \frac{4!}{\Delta_0 F_{zzzz}^0} \left. \frac{\partial(F, F_z, F_{zz})}{\partial(x, y, t)} \right|_{(0,0,0)} \neq 0. \quad (38)$$

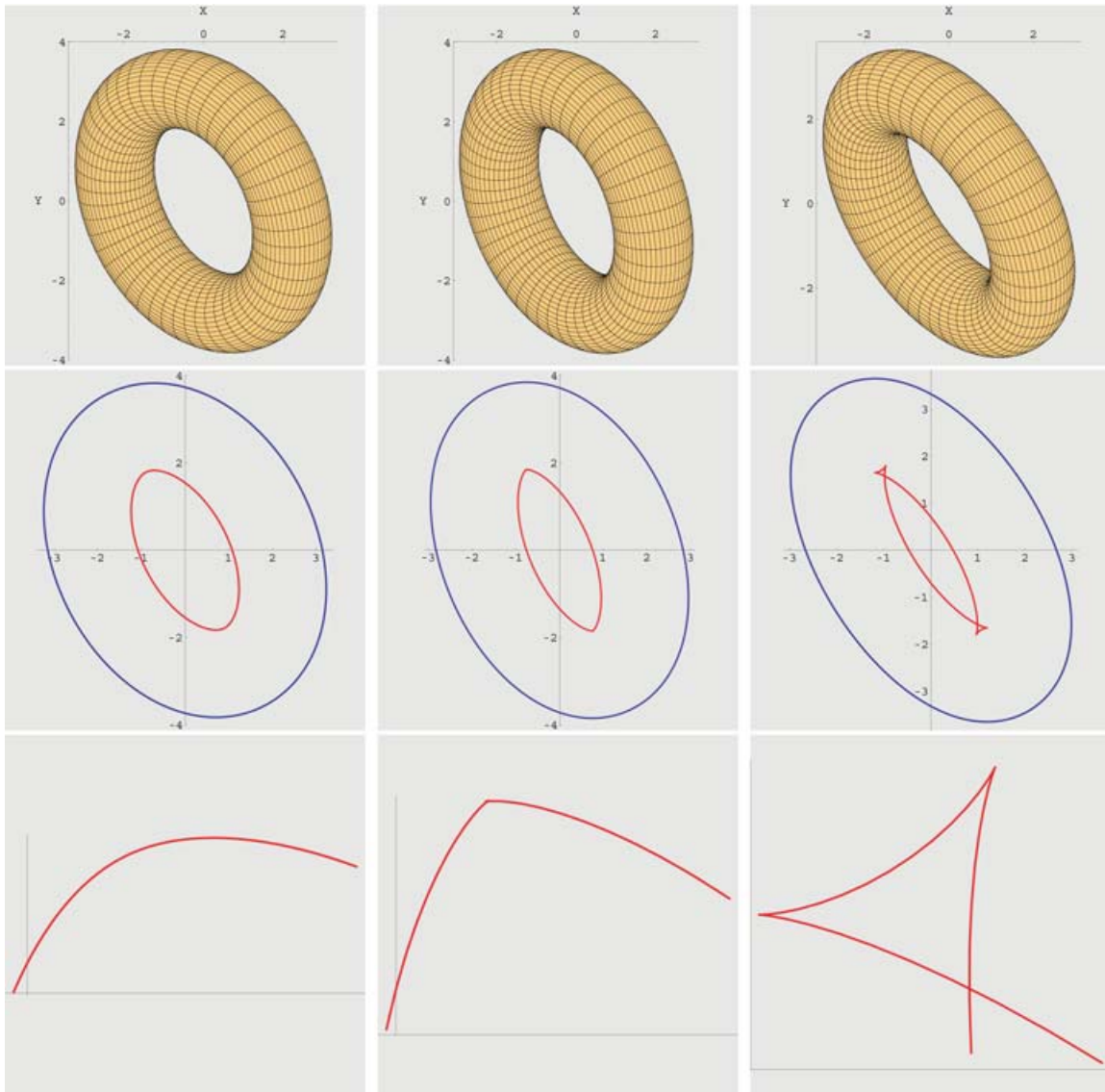


Fig. 7. A swallowtail bifurcation. Top row: a sequence of views of a smooth surface. Middle row: the corresponding apparent contours. Bottom row: blow up of the apparent contour near the bifurcation event.

In particular, there is a time-dependent change of coordinates $h^t : \mathbb{R}^2 \rightarrow \mathbb{R}^2$ that maps the apparent contour of S^t onto the apparent contour of $(G^t)^{-1}(0)$, which has a parametrization of the form $z \mapsto (x(z, t), y(z, t))$,

where

$$\begin{aligned} x(z, t) &= w^0(t)z^2 - 2w^0(t)w_x^0(t)z^3 - (3 + w^0(t)W(t))z^4 + X(z, t)z^5 \\ y(z, t) &= -2w^0(t)z + 4w^0(t)w_y^0(t)z^2 - (2 + w^0(t)W(t))z^3 + Y(z, t)z^4 \end{aligned}$$

with

$$\begin{aligned} w^0(t) &= w(0, 0, t) = \alpha t + O(t^2) \\ w_x^0(0) &= -\frac{4!}{\Delta_0 F_{zzzz}^0} \frac{\partial(F_z, F_{zz})}{\partial(x, y)} \Big|_0, \\ w_y^0(0) &= \frac{4!}{\Delta_0 F_{zzzz}^0} \frac{\partial(F, F_{zz})}{\partial(x, y)} \Big|_0, \\ W(0) &= w_x^0 + 4(w_y^0)^2. \end{aligned}$$

Remark 6.4. The parametrization of the apparent contour is of the form

$$\begin{aligned} x(z, t) &= (\alpha t + O(t^2))z^2 + O(t)z^2 - (3 + O(t))z^4 + O(z^5), \\ y(z, t) &= (-2\alpha t + O(t^2))z + O(t)z^2 - (2 + O(t^2))z^3 + O(z^4). \end{aligned}$$

For $\alpha > 0$, the evolution of the apparent contour is as that depicted in Figure 5, whereas for $\alpha < 0$, the evolution corresponds to reading the latter figure from right-to-left.

PROOF. As before, we assume that $p = (0, 0, 0)$ and $t_0 = 0$. As in the Tschirnhausen transformation, we try to transform the cubic term away by considering the equation

$$F_{zzz}(x, y, z, t) = 0. \quad (39)$$

Since $F_{zzzz}(0, 0, 0, 0) \neq 0$, there is a locally unique solution $z = \zeta(x, y, t)$ of Eq. (39) with $\zeta(0, 0, 0) = 0$. Also in this situation, Taylor expansion yields

$$F(x, y, z + \zeta(x, y, t), t) = C(U + Vz + Wz^2 + z^4 + z^5 R(x, y, z, t)),$$

where R is a smooth function, and

$$\begin{aligned} C &= C(x, y, t) = \frac{1}{4!} F_{zzzz}(x, y, \zeta(x, y, t), t), \\ U &= U(x, y, t) = F(x, y, \zeta(x, y, t), t) / C(x, y, t), \\ V &= V(x, y, t) = F_z(x, y, \zeta(x, y, t), t) / C(x, y, t), \\ W &= W(x, y, t) = \frac{1}{2} F_{zz}(x, y, \zeta(x, y, t), t) / C(x, y, t). \end{aligned}$$

In particular, $U(0, 0, 0) = 0$, $V(0, 0, 0) = 0$, $W(0, 0, 0) = 0$, and $C(0, 0, 0) \neq 0$. Since, according to Eq. (35),

$$\frac{\partial(U, V)}{\partial(x, y)} \Big|_{(0,0,0)} = \frac{4!}{F_{zzzz}^0} \frac{\partial(F, F_z)}{\partial(x, y)} \Big|_{(0,0,0,0)} = \frac{4! \Delta_0}{F_{zzzz}^0} \neq 0,$$

we see that the map $\psi : \mathbb{R}^2 \times \mathbb{R} \rightarrow \mathbb{R}^2 \times \mathbb{R}$, defined by

$$\psi(x, y, t) = (U(x, y, t), V(x, y, t), t),$$

is a local diffeomorphism, which has an inverse of the form

$$\varphi(x, y, t) = (\xi(x, y, t), \eta(x, y, t), t),$$

that is,

$$U \circ \varphi(x, y, t) = x \quad \text{and} \quad V \circ \varphi(x, y, t) = y. \quad (40)$$

Putting

$$\Phi(x, y, z, t) = (\xi(x, y, t), \eta(x, y, t), z, t),$$

we see that Φ is an admissible transformation that brings F into the normal form $G = F \circ \Phi$, which is of the form

$$G(x, y, z, t) = x + yz + w(x, y, t)z^2 + z^4 + O(|z|^5),$$

where

$$w(x, y, t) = W(\xi(x, y, t), \eta(x, y, t), t) = F_{zz}(\xi(x, y, t), \eta(x, y, t), t).$$

Therefore $w(0, 0, 0) = 0$. Furthermore,

$$w_t(0, 0, 0) = \frac{4!}{F_{zzzz}^0} (F_{xzz}^0 \xi_t^0 + F_{yzz}^0 \eta_t^0 + F_{tzz}^0).$$

From Eq. (40) we derive

$$\begin{aligned} U_x^0 \xi_t^0 + U_y^0 \eta_t^0 + U_t^0 &= 0, \\ V_x^0 \xi_t^0 + V_y^0 \eta_t^0 + V_t^0 &= 0. \end{aligned}$$

In other words,

$$\begin{pmatrix} F_x^0 & F_y^0 \\ F_{xz}^0 & F_{yz}^0 \end{pmatrix} \begin{pmatrix} \xi_t^0 \\ \eta_t^0 \end{pmatrix} = \begin{pmatrix} -F_t^0 \\ -F_{zt}^0 \end{pmatrix}.$$

Using Cramer's rule, we obtain

$$\xi_t^0 = -\frac{1}{\Delta_0} \begin{vmatrix} F_t^0 & F_y^0 \\ F_{xz}^0 & F_{yz}^0 \end{vmatrix}, \quad \text{and} \quad \eta_t^0 = -\frac{1}{\Delta_0} \begin{vmatrix} F_x^0 & F_t^0 \\ F_{xz}^0 & F_{zt}^0 \end{vmatrix}.$$

Therefore,

$$\begin{aligned} w_t^0 &= -\frac{4!}{\Delta_0 F_{zzzz}^0} \left(F_{xzz}^0 \begin{vmatrix} F_t^0 & F_y^0 \\ F_{zt}^0 & F_{yz}^0 \end{vmatrix} + F_{yzz}^0 \begin{vmatrix} F_x^0 & F_t^0 \\ F_{xz}^0 & F_{zt}^0 \end{vmatrix} - F_{tzz}^0 \begin{vmatrix} F_x^0 & F_y^0 \\ F_{xz}^0 & F_{yz}^0 \end{vmatrix} \right) \\ &= \frac{4!}{\Delta_0 F_{zzzz}^0} \begin{vmatrix} F_x^0 & F_y^0 & F_t^0 \\ F_{xz}^0 & F_{yz}^0 & F_{zt}^0 \\ F_{xzz}^0 & F_{yzz}^0 & F_{zzt}^0 \end{vmatrix} \\ &= \frac{4!}{\Delta_0 F_{zzzz}^0} \left. \frac{\partial(F, F_z, F_{zz})}{\partial(x, y, z)} \right|_0. \end{aligned} \tag{41}$$

By a similar computation, we obtain

$$w_x^0 = -\frac{4!}{\Delta_0 F_{zzzz}^0} \left. \frac{\partial(F_z, F_{zz})}{\partial(x, y, z)} \right|_0 \tag{42}$$

and

$$w_y^0 = \frac{4!}{\Delta_0 F_{zzzz}^0} \left. \frac{\partial(F, F_{zz})}{\partial(x, y, z)} \right|_0. \tag{43}$$

Finally, we can solve x and y as functions of (z, t) from the set of equations $G(x, y, z, t) = G_z(x, y, z, t) = 0$, with G as in Eq. (37). A straightforward, preferably automated, computation yields

$$\begin{aligned}
x(0, t) &= 0 \\
y(0, t) &= 0 \\
x_z(0, t) &= 0 \\
y_z(0, t) &= -2w(0, 0, t) \\
x_{zz}(0, t) &= 2w(0, 0, t) \\
y_{zz}(0, t) &= 8w(0, 0, t)w_y(0, 0, t) \\
x_{zzz}(0, t) &= -12w(0, 0, t)w_y(0, 0, t) \\
y_{zzz}(0, t) &= -12(2 + 4w(0, 0, t)w_y(0, 0, t))^2 + 2w(0, 0, t)^2w_{yy}(0, 0, t) \\
&\quad + w(0, 0, t)w_x(0, 0, t) \\
x_{zzzz}(0, t) &= 24(3 + 4w(0, 0, t)w_y(0, 0, t))^2 + 2w(0, 0, t)^2w_{yy}(0, 0, t) \\
&\quad + w(0, 0, t)w_x(0, 0, t).
\end{aligned}$$

The low-order Taylor expansions of $x(z, t)$ and $y(z, t)$, as stated in Proposition 6.3, are obtained by combining these expressions with the identities for w_t^0 , w_x^0 , and w_y^0 in Eqs. (41), (42), and (43), respectively. \square

7. INTERVAL ANALYSIS

One way to prevent rounding errors due to finite precision numbers is to use interval arithmetic. Instead of numbers, intervals containing the exact solution are computed. An *inclusion* function $\square f$ for a function $f: \mathbb{R}^m \rightarrow \mathbb{R}^n$ computes for each m -dimensional interval I (i.e., an m -box) an n -dimensional interval $\square f(I)$ such that

$$x \in I \quad \Rightarrow \quad f(x) \in \square f(I).$$

An inclusion function is *convergent* if

$$\text{width}(I) \rightarrow 0 \quad \Rightarrow \quad \text{width}(\square f(I)) \rightarrow 0,$$

where the width of an interval is the largest width of I .

For example, if $f: \mathbb{R} \rightarrow \mathbb{R}$ is the square function $f(x) = x^2$, then a convergent inclusion function is

$$\square f([a, b]) = \begin{cases} [\min(a^2, b^2), \max(a^2, b^2)], & a \cdot b < 0 \\ [0, \max(a^2, b^2)], & a \cdot b \geq 0. \end{cases}$$

Inclusion functions exist for basic operators and functions. To compute an inclusion function, it is often sufficient to replace the standard number type (e.g., double) by an interval type. Therefore, in practice, almost all functions have convergent inclusion functions that can be easily computed by using the same code, together with an interval library.

We assume there are convergent inclusion functions for our implicit function F and its derivatives, and will denote these by F (and similarly for the derivatives). From the context it will be clear when the inclusion function is meant.

Interval arithmetic can be implemented using demand-driven precision. For the interval bounds, ordinary doubles can be used for fast computation. In the rare case that the interval becomes too small for the precision of a double, a multiprecision number type can be used.

7.1 Interval Newton Method

For precision, small intervals around the required value are used. Another use of interval arithmetic is to compute function values over larger intervals. If for an implicit surface $F = 0$ and box I we have $0 \notin \square F(I)$, we can be certain that I contains no part of the surface. This observation can be extended to the Interval Newton Method that finds all roots of a function $f : \mathbb{R}^n \rightarrow \mathbb{R}^n$ in box I .

The first part of the algorithm recursively subdivides the box, discarding parts of space that contain no roots. If the boxes are “small enough,” a Newton method refines the solutions and guarantees that all roots are found. Determining when a box is small enough influences the speed of the algorithm, but is arbitrary for the guarantee to find all solutions. For the Newton step, we solve

$$f(x) + J(I)(z - x) = 0,$$

where x is the center of I , J is the Jacobian matrix of f , and $J(I)$ is the interval matrix of J over interval I , resulting in an interval Y that contains all roots z of f . This interval can be used to refine I . Also, if $Y \subset I$, there is a unique root of f in I .

We refer the reader to Hansen and Greenberg [1983] for the mathematical details. A more practical introduction can be found in Snyder [1992] or Stander and Hart [1997].

8. TRACING THE CONTOUR GENERATOR

Our goal is to approximate the contour generator by a piecewise linear curve. This initial approximation can then be maintained under some time-dependent view. To this end, the singularities of the contour generator for an evolving view or surface can be precomputed using interval analysis. Since the topology doesn't change between these singularities, the initial contour generator can be updated continuously until we reach a time wherein a singularity arises. The local model at this singularity indicates how the topology has to be updated (see Section 4).

Note that for a singularity of the contour generator of a time-dependent surface, we have

$$\begin{pmatrix} F(x, y, z, t) \\ F_z(x, y, z, t) \\ F_{zz}(x, y, z, t) \\ \Delta(x, y, z, t) \end{pmatrix} = 0$$

with Δ , as in Proposition 2.1.

These singularities can therefore be considered as the zeroes of a function from \mathbb{R}^4 to \mathbb{R}^4 . Using the Interval Newton Method, we can find all t for which a singularity occurs.

For the initial contour generator, generically, there are no singularities. The construction consists of two steps.

First, for each component of the contour generator, we have to find an initial point at which to start the tracing process. Interval analysis enables us to find points on all components of the contour generator (see the following for details). These (regular) points serve as starting points for the tracing process.

Second, we trace the component by stepping along the contour generator. For each starting point, we trace the component by moving from a point p^i to the next point p^{i+1} . We take a small step in the direction of the tangent to the contour generator at p^i . Then, we move the resulting point back to the contour generator, giving us p^{i+1} . An interval test guarantees that we stay on the same component without skipping a part. If the test fails, we decrease the step size, and try again until the interval test succeeds. If we reach the initial point p^0 , the component is fully traced.

8.1 Finding Initial Points

A tangent vector to the contour generator at p can be found by computing

$$w(p) = \nabla F(p) \wedge \nabla F_z(p) = \begin{pmatrix} F_y F_{zz} \\ -F_x F_{zz} \\ F_x F_{yz} - F_y F_{xz} \end{pmatrix}.$$

Since the components of the contour generator are bounded and closed curves, there are at least two points on each component where the x -component of $w(p)$ disappears, that is, where $F_y F_{zz} = 0$.

Let $R, S: \mathbb{R}^3 \rightarrow \mathbb{R}^3$ be the functions

$$R(p) = \begin{pmatrix} F(p) \\ F_z(p) \\ F_y(p) \end{pmatrix} \quad \text{and} \quad S(p) = \begin{pmatrix} F(p) \\ F_z(p) \\ F_{zz}(p) \end{pmatrix}.$$

The Interval Newton Method finds all roots of R and S . These roots are used to create a list of (regular) initial points.

8.2 Tracing Step

Let $T(x)$ be the normalized vector field

$$T(x) = \frac{\nabla F(x) \wedge \nabla F_z(x)}{\|\nabla F(x) \wedge \nabla F_z(x)\|}.$$

For x on the contour generator, $T(x)$ is a tangent vector at x . From p^i we first move to $q^0 = p^i + \delta T(p^i)$, where δ is the step size. To move back to the contour generator, we alternately move towards $F = 0$ and $F_z = 0$ by replacing q^i by

$$\begin{cases} q^{i+1} = q^i - \frac{F(q^i) \nabla F(q^i)}{\|\nabla F(q^i)\|^2} & \text{towards } F \\ q^{i+2} = q^{i+1} - \frac{F_z(q^{i+1}) \nabla F_z(q^{i+1})}{\|\nabla F_z(q^{i+1})\|^2} & \text{towards } F_z \end{cases}$$

until $\|q^{i+2} - q^i\|$ is sufficiently small. The resulting point is the next point on the contour generator, p^{i+1} . For this new point we perform the interval test (explained next) to determine whether $p^i p^{i+1}$ is a good approximation of the contour generator. If not, we decrease δ (e.g., by setting it to $\delta/2$), and repeat the tracing step from p^i . To prevent δ from converging to 0, we multiply it by 1.2 after each successful step.

8.3 Interval Test

For a fixed step size, there is always the possibility of accidentally jumping to another component of the contour generator or of skipping a part (Figure 8).

To assure that $p^i p^{i+1}$ is a good approximation for the contour generator, we first construct a sphere S , with center p^i , that contains p^{i+1} . Then we take the bounding box B of S :

$$B = [p_x^i - D, p_x^i + D] \times [p_y^i - D, p_y^i + D] \times [p_z^i - D, p_z^i + D],$$

where $D = \|p^{i+1} - p^i\|$. Over this box, we compute the interval

$$I = \langle T(p^i), T(B) \rangle,$$

where $T(B)$ contains all normalized vectors $\frac{\nabla F(s) \wedge \nabla F_z(t)}{\|\nabla F(s) \wedge \nabla F_z(t)\|}$ with $s, t \in B$.

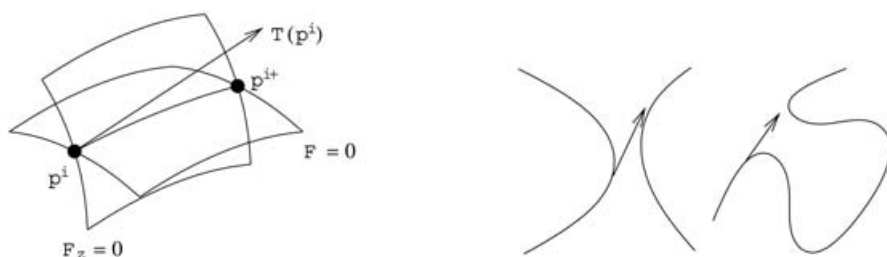


Fig. 8. (left) $T(p^i)$ is a tangent to the intersection of $F = 0$ and $F_z = 0$; (right) a fixed step size can miss part of the contour generator.

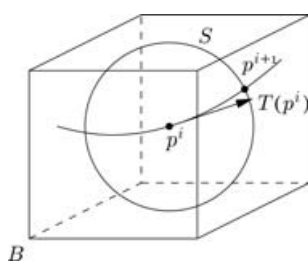


Fig. 9. The sphere containing the line segment, and its bounding box.

LEMMA 8.1. *If $I > \frac{1}{2}\sqrt{2}$, (i.e., $\forall i \in I: i > \frac{1}{2}\sqrt{2}$), then the part of the contour generator within S consists of a single component (Figure 9).*

PROOF. We define $G(x) = \langle x - p^i, T(p^i) \rangle$. The level sets of G are planes perpendicular to $T(p^i)$. Let $f: \mathbb{R}^3 \rightarrow \mathbb{R}^3$ be the function

$$f(x) = \begin{pmatrix} F(x) \\ F_z(x) \\ G(x) \end{pmatrix}.$$

Suppose there are two points, x and y , of the contour generator in B that lie in a plane perpendicular to $T(p^i)$, that is, $f(x) = f(y) = (0, 0, \theta)$ for some θ . According to the Mean Value Theorem, there are points s and t on xy where

$$\begin{pmatrix} \nabla F(s) \\ \nabla F_z(t) \\ T(p^i) \end{pmatrix} (y - x) = \begin{pmatrix} 0 \\ 0 \\ 0 \end{pmatrix}.$$

For $x \neq y$, we find that $\langle \nabla F(s) \wedge \nabla F_z(t), T(p^i) \rangle = 0$ (all vectors in a plane perpendicular to $y - x$). Since $s, t \in B$, this contradicts the interval test. Therefore, within box B , each plane perpendicular to $T(p^i)$ contains at most one point of the contour generator.

The interval condition $I > \frac{1}{2}\sqrt{2}$ implies that the angle between $T(p^i)$ and $T(x)$ is at most $\frac{\pi}{4}$ for all $x \in B$, and therefore also for $x \in \Gamma \cap B$. The contour generator lies in a cone C around $T(x)$ (Figure 10) with top angle $\frac{\pi}{2}$, for if it leaves the cone at point a , then $\langle T(p^i), T(a) \rangle$ would be smaller than $\frac{1}{2}\sqrt{2}$. It can only leave the sphere in $S \cap C$. In this part of the sphere, the contour generator cannot re-enter S because this would require an entry point b where $\langle T(p^i), T(b) \rangle < \frac{1}{2}\sqrt{2}$. Therefore, there is only a single connected component of the contour generator within sphere S . \square

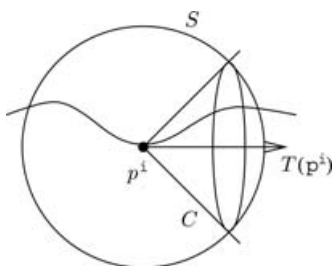


Fig. 10. The contour generator lies within a cone.

If the interval test succeeds, we can use the same sphere S to remove redundant points from the initial point list. If there are points in the list that lie within S , they must be part of the component we are tracing, so they can be discarded.

To test whether the component is fully traced, we test if the current sphere S overlaps the sphere of the initial point p^0 . If it does, testing

$$\langle p^{i+1} - p^i, p^0 - p^i \rangle > 0$$

tells us whether we are done with this component (otherwise, we have just started the trace and are still moving away from p^0).

The interval bound is valid if the center of the cube is on the contour generator. Since p^i is (in general) close to, but not on, the contour generator, in practice we take a slightly larger bound (e.g., by multiplying the radius by 1.1). Also, D should be slightly larger than $\|p^{i+1} - p^i\|$ to prevent p^{i+1} from being too close to other parts of the contour generator that are outside of S . Again, multiplying by 1.1 should suffice to prevent rounding errors.

For algorithms on implicit surfaces, it is difficult to derive a complexity bound because timing results depend not only on the complexity of the surface, but also on the behavior of the function outside the surface and on the accuracy of the convergent inclusion functions. For algebraic surfaces, it might be possible to derive the complexity in a similar manner as done by Alberti et al. [2004].

8.4 Evolving Surfaces

Time-dependent surfaces occur, for example, if the viewpoint moves along a fixed path or the surface changes shape under a continuous deformation (morphing). We assume that the transformation is also a smooth function, for example, a rotation. For a time-dependent surface $F(x, y, z, t) = 0$, there is no need to compute the initial points on the contour generator for each t . Rather, we can trace the initial points as time evolves. Recall that the initial points are zeroes of the functions $R, S: \mathbb{R}^4 \rightarrow \mathbb{R}^3$:

$$R(x, y, z, t) = \begin{pmatrix} F(x, y, z, t) \\ F_z(x, y, z, t) \\ F_y(x, y, z, t) \end{pmatrix} \quad \text{and} \quad S(x, y, z, t) = \begin{pmatrix} F(x, y, z, t) \\ F_z(x, y, z, t) \\ F_{zz}(x, y, z, t) \end{pmatrix}$$

For time-dependent surfaces, these are 1D curves in \mathbb{R}^4 . These curves can be traced similarly to the contour generator itself, that is, by stepping along the curve using a step size such that the interval inequality ($I > \frac{1}{2}\sqrt{2}$) is satisfied.

The tangent vector to the curve is perpendicular to the gradients of the three components of R and S . As time evolves, initial points are generically created and destroyed in pairs. This happens when the tangent vector is perpendicular to the t -axis. Otherwise, according to the Implicit Function Theorem, there exists a unique solution.

For R the tangent vector can be found using

$$\text{Ker} \begin{bmatrix} F_x & F_y & F_z & F_t \\ F_{xz} & F_{yz} & F_{zz} & F_{zt} \\ F_{xy} & F_{yy} & F_{yz} & F_{yt} \end{bmatrix}.$$

A solution (t_1, t_2, t_3, t_4) in the kernel with $\sum t_i = 1$ can be found by adding a row $[1, 1, 1, 1]$ to the matrix, resulting in a 4×4 matrix M , provided $\det(M) \neq 0$. Since $R(x, y, z, t) = 0$, we have $F_z = F_y = 0$. Using Cramer's rule to solve

$$\begin{pmatrix} F_x & F_y & F_z & F_t \\ F_{xz} & F_{yz} & F_{zz} & F_{zt} \\ F_{xy} & F_{yy} & F_{yz} & F_{yt} \\ 1 & 1 & 1 & 1 \end{pmatrix} \begin{pmatrix} t_1 \\ t_2 \\ t_3 \\ t_4 \end{pmatrix} = \begin{pmatrix} 0 \\ 0 \\ 0 \\ 1 \end{pmatrix},$$

we find a tangent vector for the curve:

$$\left(\begin{vmatrix} 0 & 0 & F_t \\ F_{yz} & F_{zz} & F_{zt} \\ F_{yy} & F_{yz} & F_{yt} \end{vmatrix}, - \begin{vmatrix} F_x & 0 & F_t \\ F_{xz} & F_{zz} & F_{zt} \\ F_{xy} & F_{yz} & F_{yt} \end{vmatrix}, \begin{vmatrix} F_x & 0 & F_t \\ F_{xz} & F_{yz} & F_{zt} \\ F_{xy} & F_{yy} & F_{yt} \end{vmatrix}, - \begin{vmatrix} F_x & 0 & 0 \\ F_{xz} & F_{yz} & F_{zz} \\ F_{xy} & F_{yy} & F_{yz} \end{vmatrix} \right).$$

This tangent vector is perpendicular to the t -axis if

$$\begin{pmatrix} F \\ F_z \\ F_y \\ F_x \end{pmatrix} = 0 \quad \text{or} \quad \begin{pmatrix} F \\ F_z \\ F_y \\ F_{yz}^2 - F_{yy}F_{zz} \end{pmatrix} = 0.$$

The first equality has no solutions, since the surface does not contain singularities.

Similarly, for S we have:

$$\text{Ker} \begin{bmatrix} F_x & F_y & F_z & F_t \\ F_{xz} & F_{yz} & F_{zz} & F_{tz} \\ F_{xzz} & F_{yzz} & F_{zzz} & F_{tzz} \end{bmatrix}$$

For the tangent vector of S , we find

$$\left(\begin{vmatrix} F_y & 0 & F_t \\ F_{yz} & 0 & F_{tz} \\ F_t & F_{tz} & F_{tzz} \end{vmatrix}, - \begin{vmatrix} F_x & 0 & F_t \\ F_{xz} & 0 & F_{tz} \\ F_{xzz} & F_{zzz} & F_{tzz} \end{vmatrix}, \begin{vmatrix} F_x & F_y & F_t \\ F_{xz} & F_{yz} & F_{tz} \\ F_{xzz} & F_{yzz} & F_{zzz} \end{vmatrix}, - \begin{vmatrix} F_x & F_y & 0 \\ F_{xz} & F_{yz} & 0 \\ F_{xzz} & F_{yzz} & F_{zzz} \end{vmatrix} \right).$$

This vector is perpendicular to the t -axis if

$$\begin{pmatrix} F \\ F_z \\ F_{zz} \\ F_{zzz} \end{pmatrix} = 0 \quad \text{or} \quad \begin{pmatrix} F \\ F_z \\ F_{zz} \\ F_x F_{yz} - F_y F_{xz} \end{pmatrix} = 0.$$

The first equality corresponds to swallowtail bifurcations, the second to a singularity of the contour generator.

For dynamic surfaces that depend on a single parameter, computing the 4D initial points shows us at which time steps the set of initial points for the contour generator changes. As long as the time

Table I.

Surface	Contours	Segments	Initial Pts	Tracing	Total
Tangle cube (0.095, 0.295, 1)	4	4148	3.6 s	2.2 s	5.8 s
Tangle cube (0.09, 0.29, 1)	8	3940	3.4 s	1.5 s	4.9 s
Tangle cube (0.08, 0.25, 1)	8	3184	3.0 s	1.0 s	4.0 s
Nonalg. (0.2, 0.4, 1)	62	11869	22.1 s	3.4 s	25.5 s
Nonalg. (0.8, 0.4, 1)	29	23812	75.3 s	6.8 s	82.1 s

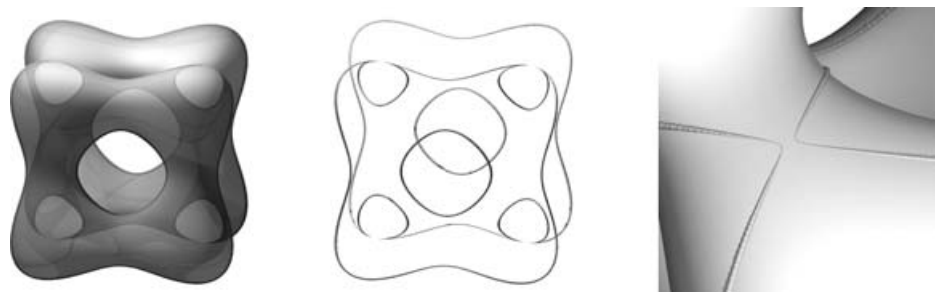


Fig. 11. Surface with contour generator, contour generator alone, and detail of the contour generator of the tangle cube $x^4 - 5x^2 + y^4 - 5y^2 + z^4 - 5z^2 + 10 = 0$. The view direction is (0.095, 0.295, 1). The contour generator is plotted as the set of spheres such that larger spheres indicate a larger step size. The actual contour generator connects the centers of these spheres. The detail shows the contour generator on the top-left of the tangle cube, shown from above.

parameter t does not pass such a time value, we can adjust the position of the current initial points to the new value of t by tracing a small part of the 4D curve. For small time steps, this requires only a small number of 4D tracing steps. The time to compute the new contour generator is therefore only slightly larger than that required for the tracing phase, removing the time required to find the initial points. When t does pass one of the precomputed values, generically, a pair of initial points of the contour generator is created or destroyed. In this case we can adjust the set of initial points by adding or removing a pair of points.

Doing more preprocessing, we could also precompute the approximation of the entire 4D curve, enabling us to find the initial points for any fixed t by intersecting this 4D curve with the t -plane.

For a single parameter function, we can handle evolving surfaces, such as level sets of an implicit function, or that move along a 1D view path. Arbitrary view directions require two parameters. In this case we also have other types of bifurcations, such as the butterfly bifurcation. How to handle the contour generators of surfaces with more than one parameter remains an open problem.

9. RESULTS

We have implemented the computation of the static contour generator using interval classes and the interval Newton solver from the *c-xsc* library.

Table I shows the results on a Pentium 2.80 GHz running Linux. The implicit surface was transformed with a shearing to change the view direction from the default (0, 0, 1). The resulting contour generators are shown in Figures 11, 12, and 13 for the tangle cube, and in Figures 14 and 15 for the nonalgebraic surface. The table shows the number of contours, the total number of line segments, and timing results for the two phases of finding the initial points, and tracing the contour generator.

At the moment, the (inclusion) functions and derivatives are hard-coded into the implementation, since we do not have an interval Newton implementation working together with automatic differentiation. A solution would be to use a code generator that outputs the inclusion functions of all derivatives. The lack of such a preprocessor makes experimenting with 4D curves tedious. However, as mentioned

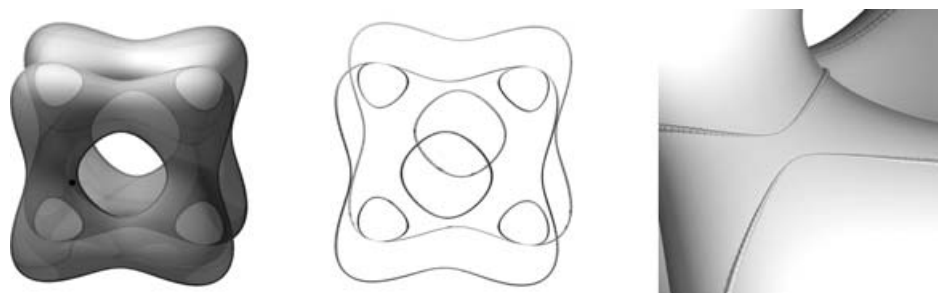


Fig. 12. Contour generator of the tangle cube, with a view direction of (0.09, 0.29, 1).

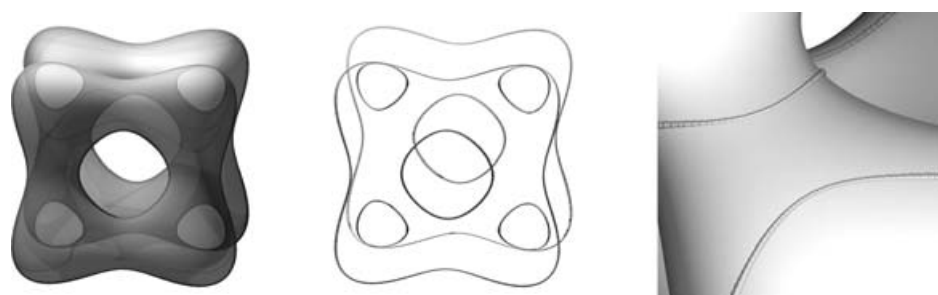


Fig. 13. Contour generator of the tangle cube, with a view direction of (0.08, 0.25, 1).

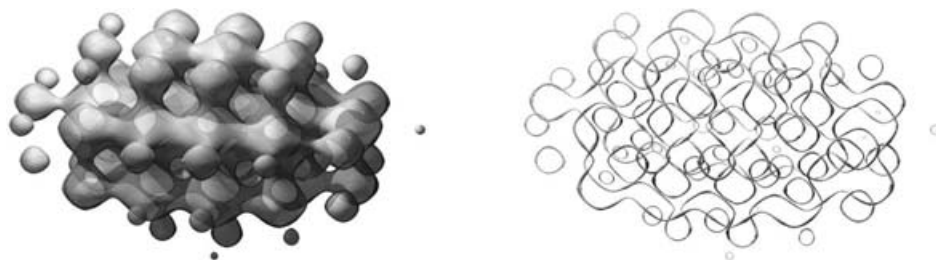


Fig. 14. Contour generator of the nonalgebraic surface $0.4(\sin(5x) + \sin(5y) + \cos(5z)) + 0.1x^2 + 0.3y^2 + 0.2z^2 - 0.5$, with a view direction of (0.2, 0.4, 1).

in the previous section, the time required for updating the contour generator for small time steps is only slightly longer than the results in Table I under “Tracing”.

The preprocessing requires computing initial points of the 4D curve. We have computed these points for the tangle cube, for the view direction moving along the 1D path $(x - tz, y - (0.2 + t)z, z)$. This path includes the views shown in Figures 11 and 12. We separately solved the three sets of equations from the previous section: $F = F_z = F_y = F_{yz}^2 - F_{yy}F_{zz} = 0$, $F = F_z = F_{zz} = F_{zzz} = 0$, and $F = F_z = F_{zz} = F_xF_{yz} - F_yF_{xz} = 0$. Table II shows the results for these three sets of equations, as well as the total time for computing the initial points of the 4D curve. The bounding box used is $[-3, 3] \times [-3, 3] \times [-3, 3]$. We solved over the intervals $[0, 1]$ and ten subintervals of width 0.1. The final row gives the sum of these ten smaller intervals.

The time for solving over the interval $[0, 1]$ is just over three hours, whereas solving over ten intervals of width 0.1 takes less than 44 minutes. This indicates that the interval Newton implementation in

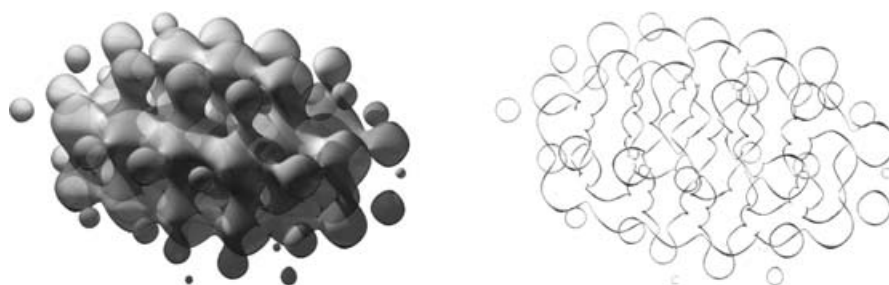


Fig. 15. Contour generator of the nonalgebraic surface with a view direction of (0.8, 0.4, 1).

Table II.

t Interval	$F_{yz}^2 - F_{yy}F_{zz}$	F_{zzz}	$F_x F_{yz} - F_y F_{xz}$	Total
[0, 1]	7894 s	977 s	1972 s	10843 s
[0.0, 0.1]	9.0 s	0.2 s	13.5 s	22.7 s
[0.1, 0.2]	23.9 s	0.7 s	21.2 s	45.8 s
[0.2, 0.3]	52.4 s	1.7 s	27.2 s	81.3 s
[0.3, 0.4]	90.8 s	4.6 s	30.8 s	126.2 s
[0.4, 0.5]	132.5 s	7.7 s	34.1 s	174.3 s
[0.5, 0.6]	181.7 s	11.4 s	40.4 s	233.5 s
[0.6, 0.7]	227.6 s	17.4 s	51.6 s	296.6 s
[0.7, 0.8]	298.2 s	33.8 s	67.3 s	399.3 s
[0.8, 0.9]	388.6 s	78.4 s	93.1 s	560.1 s
[0.9, 1.0]	476.2 s	70.7 s	127.9 s	674.8 s
10 intervals	1880.9 s	226.6 s	507.1 s	2614.6 s

Table III.

Intervals	$F_{yz}^2 - F_{yy}F_{zz}$	F_{zzz}	$F_x F_{yz} - F_y F_{xz}$	Total
Single	7894 s	977 s	1972 s	10843 s
10 time steps	1881 s	227 s	507 s	2615 s
8^4	1592 s	262 s	412 s	2266 s
16^4	989 s	161 s	277 s	1427 s
32^4	1012 s	486 s	655 s	2153 s

the c - xsc library is far from optimal. Results can be greatly improved by first subdividing the search space. The solver in c - xsc seems to switch to Newton refinement too early in the subdivision process.

To examine the effects of refinement, we split the 4D interval into N^4 subintervals, for $N = 8, 16,$ and 32 . These smaller intervals were processed by the c - xcs solver. In Table III, we repeat the results for the single interval and for splitting the time interval into ten subintervals, together with the results for the initial N^4 subdivision. An initial subdivision in 16^4 subintervals reduces the runtime by a factor of up to eight. For further subdivision, the running time increases again due to the overhead of initializing the solver. These experiments show that current implementations of the interval Newton method are far from optimal. However, optimizing generic solvers is beyond the scope of this article.

For algebraic functions such as the tangle cube, of course, other methods for solving systems of equations are available. In this case it would be much faster to use algebraic methods, instead of the generic Interval Newton method.

10. CONCLUSION AND FUTURE RESEARCH

We presented a framework for the analysis of an implicit surface near the regular and singular points of its contour generator and apparent contour, and also derived conditions for detecting changes of topology of these visibility features in generic one-parameter families of implicit surfaces.

We developed an algorithm to compute a topologically correct approximation of curves, in particular, of the initial contour generator. A dynamic step size, combined with an interval test, guarantees that no part of the contour generator is skipped.

For further experiments, we require an interval Newton method that works together with automatic differentiation or a preprocessor that generates inclusion functions for partial derivatives of the implicit function. More research needs to be done on solving systems of equations. The interval Newton method used is far from optimal. Faster solvers are required for a practical implementation of dynamic contours. Particularly, for algebraic surfaces, other methods should be considered. For this class of surfaces, it is also easier to examine the singularities by using the theory on local models. This information can be used to construct singular contours.

APPENDIX

A. SINGULARITIES OF FUNCTIONS ON SURFACES

A.1 Nondegenerate Singular Points

Consider an implicit surface $S = F^{-1}(0)$, where $F: \mathbb{R}^3 \rightarrow \mathbb{R}$ is a C^2 function. We assume that 0 is a regular value of F , so according to the Implicit Function Theorem, S is a regular C^2 -surface.

Our goal is to determine conditions which guarantee that the restriction of a C^2 function $G: \mathbb{R}^3 \rightarrow \mathbb{R}$ to the surface S has a nondegenerate singular point.

As for notation, the gradient of a function $F: \mathbb{R}^3 \rightarrow \mathbb{R}$ at $p \in \mathbb{R}^3$ will be denoted by $\nabla F(p)$. Furthermore, the *Hessian quadratic form* of a function $F: \mathbb{R}^3 \rightarrow \mathbb{R}$ at $p \in \mathbb{R}^3$ will be denoted by $H_F(p)$. Usually, we suppress the dependence on p from our notation, and denote this quadratic form by H_F . With respect to the standard Euclidean inner product, its matrix is the usual symmetric matrix whose entries are second-order partial derivatives of F . We denote partial derivatives using subscripts, for example, F_x denotes $\frac{\partial F}{\partial x}$, F_{xy} denotes $\frac{\partial^2 F}{\partial x \partial y}$, etc.

THEOREM A.1. *Let $F, G: \mathbb{R}^3 \rightarrow \mathbb{R}$ be C^2 functions, and let 0 be a regular value of F . Let p be a point on the surface $S = F^{-1}(0)$.*

(1) *p is a singular point of $G|_S$ iff there is a real number λ such that*

$$\nabla G(p) = \lambda \nabla F(p). \quad (44)$$

(2) *Furthermore, the singular point p is nondegenerate iff*

$$(H_G - \lambda H_F)|_{T_p S} \quad (45)$$

is a nondegenerate quadratic form, where λ is as in Eq. (44).

Remark. The scalar λ in Eq. (44) is traditionally called a *Lagrange multiplier*.

COROLLARY A.2. *The singularity p of $G|_S$ is nondegenerate iff the 2×2 matrix Δ , defined by Eq. (46),*

is nonsingular:

$$\Delta = V^T \cdot \left(\begin{pmatrix} G_{xx} & G_{xy} & G_{xz} \\ G_{xy} & G_{yy} & G_{yz} \\ G_{xz} & G_{yz} & G_{zz} \end{pmatrix} - \lambda \begin{pmatrix} F_{xx} & F_{xy} & F_{xz} \\ F_{xy} & F_{yy} & F_{yz} \\ F_{xz} & F_{yz} & F_{zz} \end{pmatrix} \right) \cdot V, \quad (46)$$

where λ is the Lagrange multiplier defined by Eq. (44), and V is a 3×2 matrix whose columns span the tangent space $T_p S$. Here, all first- and second-order derivatives are evaluated at p . Furthermore, for $G|S$, the singular point p is a maximum or minimum if $\det(\Delta) > 0$, and a saddle point if $\det(\Delta) < 0$.

In particular, we may take $V = X$, $V = Y$, or $V = Z$ if $F_x(p) \neq 0$, $F_y(p) \neq 0$, or $F_z(p) \neq 0$, respectively, where

$$X = \begin{pmatrix} F_y & F_z \\ -F_x & 0 \\ 0 & -F_x \end{pmatrix}, Y = \begin{pmatrix} -F_y & 0 \\ F_x & F_z \\ 0 & -F_y \end{pmatrix}, Z = \begin{pmatrix} -F_z & 0 \\ 0 & -F_z \\ F_x & F_y \end{pmatrix}. \quad (47)$$

PROOF OF THEOREM A.1. (1) Saying that p is a singular point of $G|S$ is equivalent to $dG_p(v) = 0$ for all $v \in T_p S$. Since $T_p S = \ker dF_p$, we see that this is equivalent to the existence of a scalar λ such that $dG_p = \lambda dF_p$.

(2) Since 0 is a regular value of F , we have $\nabla F(p) \neq 0$. We assume that $F_x(p) \neq 0$, and argue similarly in case $F_y(p) \neq 0$ or $F_z(p) \neq 0$. Furthermore, assume that $p = (0, 0, 0)$. According to the Implicit Function Theorem, there is a unique local solution $x = f(y, z)$, with $f(0, 0) = 0$, of the equation $F(x, y, z) = 0$. Implicit differentiation yields

$$F_x f_y + F_y = 0, \quad (48)$$

$$F_x f_z + F_z = 0, \quad (49)$$

where f_y and f_z are evaluated at (y, z) and F_x , F_y , and F_z are evaluated at $(f(y, z), y, z)$. Similarly,

$$F_{xx} f_y^2 + 2F_{xy} f_y + F_{yy} + F_x f_{yy} = 0. \quad (50)$$

Similar identities are obtained by differentiating Eq. (48) with respect to y , and Eq. (49) with respect to z .

Using y and z as local coordinates on S , we obtain the following expression of $G|S$ with respect to these local coordinates:

$$g(y, z) = G(f(y, z), y, z).$$

Differentiating this identity twice with respect to y , we obtain

$$g_{yy} = G_{xx} f_y^2 + 2G_{xy} f_y + G_{yy} + G_x f_{yy}. \quad (51)$$

Since $F_x(p) \neq 0$, we solve f_{yy} from Eq. (50), and plug the resulting expression into (51) to get

$$g_{yy} = (G_{xx} - \lambda F_{xx}) f_y^2 + 2(G_{xy} - \lambda F_{xy}) f_y + (G_{yy} - \lambda F_{yy}), \quad (52)$$

where

$$\lambda = \frac{G_x}{F_x}$$

is the Lagrange multiplier (see Eq. (44)). We rewrite (52) as

$$\begin{aligned} g_{yy} &= (f_y \ 1 \ 0)(H_G - \lambda H_F) \begin{pmatrix} f_y \\ 1 \\ 0 \end{pmatrix} \\ &= \frac{1}{F_x^2} (F_y \ -F_x \ 0)(H_G - \lambda H_F) \begin{pmatrix} F_y \\ -F_x \\ 0 \end{pmatrix}. \end{aligned}$$

We similarly derive

$$g_{yz} = \frac{1}{F_x^2} (F_y \ -F_x \ 0)(H_G - \lambda H_F) \begin{pmatrix} F_z \\ 0 \\ -F_x \end{pmatrix},$$

and

$$g_{zz} = \frac{1}{F_x^2} (F_z \ 0 \ -F_x)(H_G - \lambda H_F) \begin{pmatrix} F_z \\ 0 \\ -F_x \end{pmatrix}.$$

Since the vectors $(F_y, -F_x, 0)$ and $(F_z, 0, -F_x)$ span the tangent space $T_p S$, we see that

$$\begin{pmatrix} g_{yy} & g_{yz} \\ g_{yz} & g_{zz} \end{pmatrix} = \frac{1}{F_x^2} \Delta.$$

B. THE MORSE LEMMA WITH PARAMETERS

The Morse Lemma gives a normal form for a smooth function in a neighborhood of a nondegenerate critical point. We discuss an extension of this result to functions that depend on parameters. We refer to Arnol'd [1976] for a proof. Let $F : \mathbb{R}^n \times \mathbb{R}^k \rightarrow \mathbb{R}$ be a smooth map, and let the function $f : \mathbb{R}^n \rightarrow \mathbb{R}$, defined by $f(x) = F(x, 0)$, have a nondegenerate singularity at $p \in \mathbb{R}^n$. Then, the function $F_\mu : \mathbb{R}^n \rightarrow \mathbb{R}$ has a nondegenerate singularity p_μ , which depends smoothly on $\mu \in \mathbb{R}^k$, and coincides with p for $\mu = 0$. In fact, the singular point $x = p_\mu$ is a solution of the system of equations

$$\frac{\partial F}{\partial x_1}(x, \mu) = \dots = \frac{\partial F}{\partial x_n}(x, \mu) = 0.$$

The Jacobian determinant of this system at $(x, \mu) = (p, 0)$ is equal to the determinant of the Hessian matrix of f at 0, which is nonzero. Therefore, the Implicit Function Theorem guarantees the existence and uniqueness of the local solution p_μ .

PROPOSITION B.1. *There is a local diffeomorphism $\Phi : \mathbb{R}^n \times \mathbb{R}^k \rightarrow \mathbb{R}^n \times \mathbb{R}^k$, defined on a neighborhood of $(p, 0)$, of the form*

$$\Phi(x, \mu) = (\varphi(x, \mu), \mu),$$

such that

$$F \circ \Phi(x, \mu) = \sigma_1 x_1^2 + \dots + \sigma_n x_n^2 + F(p_\mu, \mu),$$

where $\sigma_i = \pm 1$, $i = 1, \dots, n$, defines the signature of the quadratic part of f at p .

The proof of the Morse Lemma with parameters is completely similar to the proof of the “regular” Morse Lemma.

C. NORMAL FORM OF A WHITNEY FOLD

C.1 Fold Points of Good Mappings

A celebrated theorem by Whitney [1955] states that generic mappings of the plane into the plane have only two types of singular points, namely, folds or cusps. In this section we discuss a normal form for such a mapping in the neighborhood of a fold point, and sketch a method for actually computing such a normal form.

Let $f : \mathbb{R}^2 \rightarrow \mathbb{R}^2$ be a mapping, and let $J : \mathbb{R}^2 \rightarrow \mathbb{R}$ be its Jacobian determinant. More precisely, if $f(x, y) = (u(x, y), v(x, y))$, then

$$J = u_x v_y - u_y v_x.$$

The mapping f is called *good* if $J(p) \neq 0$ or $\nabla J(p) \neq 0$, at every point $p \in \mathbb{R}^2$. In other words, the system of equations

$$J(x, y) = J_x(x, y) = J_y(x, y) = 0 \tag{53}$$

has no solutions in \mathbb{R}^2 . It can be proven that this condition is independent of the choice of coordinates.

Whitney proves that generically, a map from plane into plane is good. Intuitively, this may seem to follow from the observation that generic systems of three equations in two unknowns do not have a solution. However, it is not obvious that Eq. (53) is a generic system. A proof can be given using Thom’s transversality theorem.

Consequently, the singular set $S_1(f) = J^{-1}(0)$ of a good map consists of a number of disjoint regular curves in the plane. This is a straightforward consequence of the Implicit Function Theorem, since the gradient of J is nonzero at every point of $S_1(f)$.

Furthermore, at a singular point p , at least one of the partial derivatives of the component functions of f is nonzero, that is

$$(u_x(p), u_y(p), v_x(p), v_y(p)) \neq (0, 0, 0, 0). \tag{54}$$

In particular, the rank of the derivative df_p at a singular point is one, or equivalently, the kernel of df_p is 1D. A singular point p of a good map f is called a *fold point* Golubitsky and Guillemin [1973] if

$$T_p S_1(f) \oplus \text{Ker} df_p = \mathbb{R}^2. \tag{55}$$

Note that the tangent space $T_p S_1(f)$ is well-defined, since $S_1(f)$ is a regular curve. Whitney’s [1955] version of Eq. (55) is slightly different: if w is a nonzero tangent vector at p to $S_1(f)$, then the directional derivative of f in direction w is nonzero, that is, $\nabla_w f(p) \neq 0$. Obviously, the two versions are equivalent, and, more importantly, neither depends on a particular choice of coordinates. The latter observation follows from Lemma C.1.

LEMMA C.1. *Let f be a good map, $\varphi : \mathbb{R}^2 \rightarrow \mathbb{R}^2$ an invertible nonsingular map, and $g = f \circ \varphi$. Then,*

- (i) $S_1(g) = \varphi^{-1}(S_1(f))$;
- (ii) $g(S_1(g)) = f(S_1(f))$;
- (iii) g is a good map; and
- (iv) p is a fold point of g iff $\varphi(p)$ is a fold point of f .

PROOF. Let J and \tilde{J} be the Jacobian determinants of f and g , respectively. Since

$$dg_p = df_{\varphi(p)} \circ d\varphi_p, \quad (56)$$

we see that

$$\tilde{J}(p) = J(\varphi(p)) \cdot \det d\varphi_p. \quad (57)$$

Therefore, $\varphi(\tilde{J}^{-1}(0)) = J^{-1}(0)$, which is equivalent to the first claim. The second claim is an immediate consequence of the first. To prove the third claim, let $p \in S_1(g)$, that is, $\tilde{J}(p) = 0$. Then Eq. (57) implies $J(\varphi(p)) = 0$. Thus, applying the product rule to (57) yields

$$d\tilde{J}_p = \det d\varphi_p \circ dJ_{\varphi(p)} \circ d\varphi_p. \quad (58)$$

Since $d\varphi_p$ is invertible, we see that the scalar $\det d\varphi_p$ is nonzero, hence that

$$d\tilde{J}_p \neq 0 \text{ iff } dJ_{\varphi(p)} \neq 0.$$

This proves the third claim. Finally, observe that Eq. (56) implies

$$d\varphi_p(\text{Kerd}g_p) = \text{Ker}df_{\varphi(p)}, \quad (59)$$

and that Eq. (58) implies

$$d\varphi_p(\text{Kerd}\tilde{J}_p) = \text{Kerd}J_{\varphi(p)}. \quad (60)$$

Since $\text{Kerd}\tilde{J}_p = T_p S_1(g)$ and $\text{Kerd}J_{\varphi(p)} = T_{\varphi(p)} S_1(f)$, we conclude from Eqs. (59) and (60) that

$$T_p S_1(g) \oplus \text{Kerd}g_p = \mathbb{R}^2 \text{ iff } T_{\varphi(p)} S_1(f) \oplus \text{Ker}df_{\varphi(p)} = \mathbb{R}^2.$$

In other words, p is a fold point of g iff $\varphi(p)$ is a fold point of f . This concludes the proof of the fourth claim. \square

For later use, we isolate the following result.

LEMMA C.2. *Let $f : \mathbb{R}^2 \rightarrow \mathbb{R}^2$ be a good map with component functions $u, v : \mathbb{R}^2 \rightarrow \mathbb{R}$ and Jacobian determinant $J : \mathbb{R}^2 \rightarrow \mathbb{R}$. The following statements are equivalent:*

- (i) p is a fold point of f ;
- (ii) $W_p \neq (0, 0)$, where

$$W_p = (\langle \nabla u(p), \nabla J(p)^\perp \rangle, \langle \nabla v(p), \nabla J(p)^\perp \rangle).$$

In either case, W_p is a tangent vector of the regular curve $f(S_1(f))$ at p .

PROOF. Since f is good, $J^{-1}(0) = S_1(f)$ is a regular curve containing p . Its tangent vector at p is $\nabla J(p)^\perp$.

Since df_p has rank one, we have $\nabla u(p) \neq (0, 0)$ or $\nabla v(p) \neq (0, 0)$. Assume the former inequality holds. Then, there is a real constant c such that

$$\nabla v(p) = c\nabla u(p).$$

Now

$$df_p(W) = (\langle \nabla u(p), W \rangle, \langle \nabla v(p), W \rangle) \quad (61)$$

for $W \in \mathbb{R}^2$, so $df_p(\nabla u(p)^\perp) = (0, 0)$. Hence $\text{Ker}df_p = \mathbb{R}\nabla u(p)^\perp$.

It now follows that Eq. (55) holds iff $\nabla u(p)^\perp$ is not parallel to $\nabla J(p)^\perp$ or iff $\langle \nabla u(p), \nabla J(p)^\perp \rangle \neq 0$. Similarly, if $\nabla v(p) \neq 0$, then (55) is equivalent to $\langle \nabla v(p), \nabla J(p)^\perp \rangle \neq 0$. In either case, $W_p \neq 0$. This proves the equivalence of (i) and (ii).

To prove that W_p is tangent to $f(S_1(f))$ at p , let $s \mapsto (x(s), y(s))$ be a regular parametrization of $J^{-1}(0)$, with $(x(0), y(0)) = p$ and $(x'(0), y'(0)) = \nabla J(p)^\perp$. Then, $\alpha(s) = f(x(s), y(s))$ is a parametrization of $f(J^{-1}(0))$, and, in view of Eq. (61), we have

$$\alpha'(0) = df_p(\nabla J(p)^\perp) = W_p. \quad (62)$$

□

C.2 Normal Form of a Good Map Near a Fold Point

Our goal is to obtain a simple form of a good map near a fold point. Such a *normal form* can be obtained by applying a change of coordinates on the *domain* of the map, its range, or both. We start by applying only changes of coordinates on the domain of the map.

PROPOSITION C.3. *Let $f : \mathbb{R}^2 \rightarrow \mathbb{R}^2$ be a good map with component functions $u, v : \mathbb{R}^2 \rightarrow \mathbb{R}$ and Jacobian determinant $J : \mathbb{R}^2 \rightarrow \mathbb{R}$. Let $p = (0, 0)$ be a fold point of f with $f(p) = (0, 0)$. The following properties are equivalent:*

- (i) $f(J^{-1}(0))$ is transversal to the y -axis at $f(p)$;
- (ii) $\nabla u(p) \neq (0, 0)$; and
- (iii) there is a local change of coordinates $\varphi : \mathbb{R}^2 \rightarrow \mathbb{R}^2$, with $\varphi(0, 0) = p$ such that

$$f \circ \varphi(x, y) = (x, \sigma y^2 + \alpha(x)), \quad (63)$$

where $\sigma = \text{sign}(\langle \nabla u(p), \nabla J(p)^\perp \rangle) = \pm 1$, and $\alpha : \mathbb{R} \rightarrow \mathbb{R}$ is a smooth function with $\alpha(0) = 0$.

Remark C.4. If $g = f \circ \varphi$, we shall say that φ brings f into the form g . The righthand-side of Eq. (63) will be considered normal form. The transformations bringing the mapping into normal form should be *computationally feasible*. Therefore, we shall be very precise about each and every step we take.

PROOF OF PROPOSITION C.3. The equivalence of conditions (i) and (ii) follows from Lemma C.2. To see that (iii) implies (i), let $g = f \circ \varphi$. Then $f(S_1(f)) = g(S_1(g))$, according to Lemma C.1(ii). Since $g(S_1(g)) = \{(x, \alpha(x)) \mid x \in \mathbb{R}^2\}$, the first claim follows. So it remains to prove that (ii) implies (iii). The proof follows in two steps. We assume that $p = (0, 0)$.

Step 1. There is a local change of coordinates, bringing f into one of the forms $g(x, y) = (x, V(x, y))$. To see this, we first consider the case

$$u_x^0 \neq 0, \quad (64)$$

where the notation is as in Section C.1. Here the superscript 0 indicates that the corresponding function has to be evaluated at $p = (0, 0) \in \mathbb{R}^2$. In view of Eq. (64), the change of coordinates $\psi : \mathbb{R}^2 \rightarrow \mathbb{R}^2$, defined by

$$\psi(x, y) = (u(x, y), y),$$

is nonsingular. Let φ be the inverse of ψ , thus $\varphi(x, y) = (\xi, \eta)$ iff $\eta = y$ and

$$u(\xi, y) - x = 0. \quad (65)$$

Let $\xi = \xi(x, y)$ be the locally unique solution of Eq. (65) with $\xi(0, 0) = 0$. Then

$$\varphi(x, y) = (\xi(x, y), y),$$

and

$$f \circ \varphi(x, y) = (x, V(x, y)) \text{ with } V(x, y) = v(\xi(x, y), y).$$

If $u_x^0 = 0$, then condition (ii) implies that $u_y^0 \neq 0$. This case is reduced to Eq. (64) by first applying the transformation $(x, y) \mapsto (y, x)$.

Step 2. If $f(x, y) = (x, V(x, y))$ is a good map with a fold point at $(0, 0)$, then there is a local change of coordinates, bringing g into the form $g(x, y) = (x, \pm y^2 + \alpha(x))$, where $\alpha : \mathbb{R} \rightarrow \mathbb{R}$ is a smooth function with $\alpha(0) = 0$.

Since

$$df_{(x,y)} = \begin{pmatrix} 1 & 0 \\ V_x & V_y \end{pmatrix},$$

we see that $(0, 0)$ is a singular point of f iff

$$V_y^0 = 0. \quad (66)$$

In this case, $\text{Ker}df_{(0,0)}$ is the span of vector $(0, 1)$. Furthermore, $J = V_y$, so the fact that f is a good mapping implies in particular that $\nabla J(0, 0) = (V_{xy}^0, V_{yy}^0) \neq (0, 0)$. A nonzero tangent vector to $S_1(f) = J^{-1}(0)$ at $(0, 0)$ is $\nabla J(0, 0)^\perp = (-V_{yy}^0, V_{xy}^0)$. It is now easy to see that condition (55) is equivalent to

$$V_{yy}^0 \neq 0. \quad (67)$$

Since also $V(0, 0) = 0$, we apply the Morse Lemma with parameters to bring the function V into normal form. More precisely, there is a local change of parameters $\varphi : \mathbb{R}^2 \rightarrow \mathbb{R}^2$ of the form $\varphi(x, y) = (x, \Phi(x, y))$ such that

$$V \circ \varphi(x, y) = \pm y^2 + \alpha(x),$$

where α is a smooth function with $\alpha(0) = 0$. It is now obvious that $f \circ \varphi$ is the desired normal form.

Concatenating Steps 1 and 2 concludes the proof. \square

COROLLARY C.5. *If $f : \mathbb{R}^2 \rightarrow \mathbb{R}^2$ is a good mapping with a fold point at p , then there is a local change of coordinates $\varphi : \mathbb{R}^2 \rightarrow \mathbb{R}^2$, near $(0, 0)$, with $\varphi(0, 0) = p$, and a local change of coordinates $\psi : \mathbb{R}^2 \rightarrow \mathbb{R}^2$ with $\psi(f(p)) = (0, 0)$ such that*

$$\psi \circ f \circ \varphi(x, y) = (x, y^2).$$

PROOF. Applying Proposition C.3, we may assume that $f(x, y) = (x, \pm y^2 + \alpha(x))$ or $f(x, y) = (\pm x^2 + \alpha(y), y)$. In the first case, take $\psi(x, y) = (x, \pm(y - \alpha(x)))$. Then $\psi \circ f(x, y) = (x, y^2)$. The second case is treated similarly. \square

Remark C.6. In Step 1 of the proof of Proposition C.3, in case $u_x \neq 0$, near $p = (0, 0)$ we define the function V by $V(x, y) = v(\xi(x, y), y)$, where $\xi = \xi(x, y)$ is the solution of $u(\xi, y) - x = 0$. The derivatives V_y and V_{yy} can be computed from this definition in a straightforward way:

$$V_y = u_x \xi_y + v_y = u_x \left(-\frac{u_y}{u_x} \right) + v_y = \frac{J}{u_x},$$

where all functions in the righthand-sides are evaluated at $(\xi(x, y), y)$. Since $J(0, 0) = 0$, we obtain

$$V_{yy}(0, 0) = \frac{(J_x^0 \xi_y^0 + J_y^0) u_x^0}{(u_x^0)^2} = \frac{-u_y^0 J_x^0 + u_x^0 J_y^0}{(u_x^0)^2}.$$

Therefore, $V_{yy}(0, 0) \neq 0$ iff $\langle \nabla u(0, 0), \nabla J(0, 0)^\perp \rangle \neq 0$ iff the vectors $\nabla u(0, 0)^\perp$ and $\nabla J(0, 0)^\perp$ are not parallel.

We claim that $\nabla u(0, 0)^\perp = (-u_y^0, u_x^0)$ is a nonzero vector in $\text{Ker} df_0$. Indeed, since df_0 has rank one, we see that $\nabla v(0, 0) = c \nabla u(0, 0)$ for some real constant c . Therefore

$$\begin{pmatrix} u_x^0 & u_y^0 \\ v_x^0 & v_y^0 \end{pmatrix} \begin{pmatrix} -u_y^0 \\ u_x^0 \end{pmatrix} = \begin{pmatrix} 0 \\ 0 \end{pmatrix},$$

which proves our claim. Since $\nabla J(0, 0)^\perp$ is tangent to $J^{-1}(0) = S_1(f)$, we see that the latter condition is equivalent to Eq. (55). In other words, $V_{yy}(0, 0) \neq 0$ iff condition (55) holds. This is what we also observed in Step 2 of the proof of Proposition C.3.

C.3 Introducing Parameters

If f depends on an additional parameter t , we can still obtain a normal form like that of Eq. (63), provided we let both the transformation φ and function α depend on this new parameter. More precisely, consider a family of maps $f_t : \mathbb{R}^2 \rightarrow \mathbb{R}^2$ that depends smoothly on the parameter $t \in \mathbb{R}$ such that f_0 satisfies any of the conditions (i), (ii), or (iii) of Proposition C.3. With this family we associate the map $F : \mathbb{R}^2 \times \mathbb{R} \rightarrow \mathbb{R}^2$ defined by $F(x, t) = f_t(x)$. Then, there is a one-parameter family $\Phi : \mathbb{R}^2 \times \mathbb{R} \rightarrow \mathbb{R}^2 \times \mathbb{R}$ of local coordinate transformations of the form

$$\Phi(x, y, t) = (\varphi_t(x, y), t)$$

such that

$$F \circ \Phi(x, y, t) = (x, \sigma y^2 + \alpha(x, t)). \quad (68)$$

The latter identity may be rephrased as

$$f_t \circ \varphi_t(x, y) = (x, \sigma y^2 + \alpha(x, t)).$$

The image of the fold curve of f_t is $f_t(S_1(f_t)) = \{(x, \alpha(x, t)) \mid x \in \mathbb{R}\}$. The point of intersection of this curve with the y -axis, namely, $(0, \alpha(0, t))$, passes through the origin with speed α_t^0 (Here we consider t as time). To express this velocity in terms of f_t , let $u(x, y, t)$ and $v(x, y, t)$ be the component functions of $F(x, y, t)$.

LEMMA C.7. *If $u_x(p, 0) \neq 0$, then*

$$\alpha_t^0 = \frac{1}{u_x(p, 0)} \frac{\partial(u, v)}{\partial(x, t)}(p, 0),$$

and if $u_y(p, 0) \neq 0$, then

$$\alpha_t^0 = \frac{1}{u_y(p, 0)} \frac{\partial(u, v)}{\partial(y, t)}(p, 0).$$

PROOF. Let $\Phi(x, y, t) = (\xi(x, y, t), \eta(x, y, t))$. Then, Eq. (68) reduces to

$$\begin{aligned} u(\xi(x, y, t), \eta(x, y, t), t) &= x, \\ v(\xi(x, y, t), \eta(x, y, t), t) &= \sigma y^2 + \alpha(x, t). \end{aligned}$$

Differentiating the latter identity with respect to t and evaluating at $(p, 0)$ yields

$$\begin{aligned} u_x^0 \xi_t^0 + u_y^0 \eta_t^0 + u_t^0 &= 0, \\ v_x^0 \xi_t^0 + v_y^0 \eta_t^0 + v_t^0 &= \alpha_t^0. \end{aligned} \tag{69}$$

Since the second condition of Proposition C.3 holds, that is, $(u_x^0, u_y^0) \neq (0, 0)$, there is a scalar constant c such that $(u_x^0, u_y^0) = c(v_x^0, v_y^0)$. Therefore, Eq. (69) implies that

$$\alpha_t^0 = v_t^0 - cu_t^0 = \frac{1}{u_x^0} (u_x^0 v_t^0 - v_x^0 u_t^0).$$

If $u_y^0 \neq 0$, the second identity is derived similarly. \square

Remark C.8. Lemma C.7 implies that $\alpha_t^0 \neq 0$ iff the matrix

$$\begin{pmatrix} u_x^0 & u_y^0 & u_t^0 \\ v_x^0 & v_y^0 & v_t^0 \end{pmatrix}$$

has rank two. Furthermore, since $u_x^0 v_y^0 - u_y^0 v_x^0 = 0$, it follows that

$$u_y^0 \begin{vmatrix} u_x^0 & u_t^0 \\ v_x^0 & v_t^0 \end{vmatrix} = u_x^0 \begin{vmatrix} u_y^0 & u_t^0 \\ v_y^0 & v_t^0 \end{vmatrix}.$$

In view of Lemma C.7, both sides of this equality are equal to $u_x^0 u_y^0 \alpha_t^0$.

REFERENCES

- ALBERTI, G., COMPTE G., AND MOURRAIN, B. 2004. Meshing implicit algebraic surfaces: The smooth case. Tech. rep. 5405, INRIA Sophia-Antipolis.
- ALLIEZ, P., LAURENT, N., SANSON, H., AND SCHMITT, F. 2001. Efficient view-dependent refinement of 3d meshes using sqrt(3)-subdivision. To appear in *the Visual Computer*.
- ARNOLD, V. I. 1976. Wave front evolution and equivariant Morse lemma. *Comm. Pure Appl. Math.* 29, 557–582.
- ARNOLD, V. I. 1986. *Catastrophe Theory*. Springer-Verlag, Berlin.
- BAREQUET, G., DUNCAN, C. A., GOODRICH, M. T., KUMAR, S., AND POP, M. 1999. Efficient perspective-accurate silhouette computation. In *Proceedings of the 15th Annual ACM Symposium on Computer Geometry*. 417–418.
- BLOOMENTHAL, J. 1997. *Introduction to Implicit Surfaces*. Morgan-Kaufmann, San Fransisco, CA.
- BREMER, D. J. AND HUGHES, J. F. 1998. Rapid approximate silhouette rendering of implicit surfaces. In *Proceedings of the Implicit Surfaces Conference*. 155–164.
- BRUCE, J. W. 1984. Seeing—The mathematical viewpoint. *The Mathematical Intelligencer* 6, 18–25.
- BRUCE, J. W. AND GIBLIN, P. J. 1985. Outlines and their duals. *Proc. London Math. Soc.* 3, 50, 552–570.
- CIPOLLA, R. AND GIBLIN, P. J. 2000. *Visual Motion of Curves and Surfaces*. Cambridge University Press, New York.
- FOMENKO, A. T. AND KUNII, T. L. 1997. *Topological Modeling for Visualization*. Springer-Verlag, Berlin.
- GOLUBITSKY, M. AND GUILLEMIN, V. 1973. *Stable Mappings and Their Singularities*, vol. 14, *Graduate Texts in Mathematics*. Springer-Verlag, Berlin.
- GU, X., GORTLER, S. J., HOPPE, H., McMILLAN, L., BROWN, B. J., AND STONE, A. D. 1999. Silhouette mapping. Tech. Rep. TR-1-99, Department of Computer Science, Harvard University (Mar.).
- HANSEN, E. R. AND GREENBERG, R. I. 1983. An interval Newton method. *Appl. Math Comput.* 12, 89–98.
- HEARN, D. AND BAKER, M. P. 1994. *Computer Graphics*, 2nd ed. Prentice-Hall, Englewood Cliffs, NJ.
- HOFFMAN, C. M. 1989. *Geometric and Solid Modeling*. Morgan-Kaufmann, San Fransisco, CA.
- KOENDERINK, J. J. 1990. Solid shape. In *Artificial Intelligence*. MIT Press, Cambridge, MA.
- MARKOSIAN, L., KOWALSKI, M. A., TRYCHIN, S. J., BOURDEV, L. D., GOLDSTEIN, D., AND HUGHES, J. F. 1997. Real-Time nonphotorealistic rendering. In *Proceedings of the 24th Annual Conference on Computer Graphics and Interactive Techniques*. 415–420.

- MILNOR, J. 1963. *Morse Theory*. In *Annals of Mathematics Studies, vol. 51*. Princeton University Press, Princeton, NJ.
- OPALACH, A. AND MADDOCK, S. C. 1995. An overview of implicit surfaces. In *Introduction to Modelling and Animation Using Implicit Surfaces*. 1.1–1.13.
- PLATINGA, S. AND VEGTER, G. 2003. Contour generators of evolving implicit surfaces. In *Proceedings of the Solid Modeling Conference*. 23–32.
- SNYDER, J. M. 1992. Interval analysis for computer graphics. In *Proceedings of the 19th Annual Conference on Computer Graphics and Interactive Techniques*. 121–130.
- STANDER, B. T. AND HART, J. C. 1997. Guaranteeing the topology of an implicit surface polygonization for interactive modeling. In *Proceedings of the 24th Annual Conference on Computer Graphics and Interactive Techniques*. 279–286.
- WHITNEY, H. 1955. On singularities of mappings of Euclidean spaces I, mappings of the plane into the plane. *Ann. Math.* 62, 374–410.

Received March 2004; revised January 2006; accepted August 2006